

Optimising power-to-gas integration with wastewater treatment and biogas: A techno-economic assessment of CO₂ and by-product utilisation

Linus Engstam^{a,*}, Leandro Janke^b, Cecilia Sundberg^a, Åke Nordberg^a

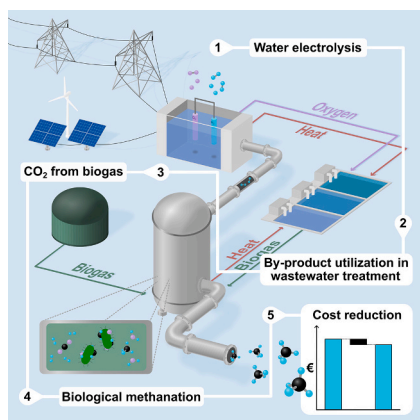
^a Department of Energy and Technology, Swedish University of Agricultural Sciences, Box 7032, 750 07 Uppsala, Sweden

^b Agora Energiewende, Anna-Louisa-Karsch-Str. 2, 10178 Berlin, Germany

HIGHLIGHTS

- An hourly-based model of a locally integrated PtG system was developed.
- Configuration optimisation led to minimum production cost of 194.6 €/MWh.
- Heat and oxygen use altered production costs by −2 % and + 1 %, respectively.
- The system produced heat in excess, but could not meet oxygen demand.
- Biogas upgrading via PtG increased costs by 54 % compared with amine scrubbing.

GRAPHICAL ABSTRACT



ARTICLE INFO

Keywords:

Power-to-Gas
Biogas
Wastewater treatment
By-product utilisation
Optimisation
Techno-economic assessment

ABSTRACT

Production of electrolytic hydrogen and its conversion to methane, also known as power-to-gas (PtG), could play a key role in the transition towards a defossilised energy system. Integration of PtG technology with wastewater treatment and co-digestion presents an opportunity to produce low-carbon methane while simultaneously upgrading biogas, recycling biogenic carbon dioxide and utilising process by-products (heat and oxygen). A model of such an integrated system was developed using real plant data to assess the techno-economic performance through simulation of hourly operation and configuration optimisation. The integrated concept was demonstrated to be a promising option for increasing efficiency and reducing costs and emissions in the PtG system. By-product utilisation increased net energy efficiency from 52.3 to 59.7 %_{HHV}, leading to a reduction in levelised cost of PtG (LCO_{PtG}) of 1.0 % and in net specific emissions of 28.3 % and 2.2 % based on average and marginal grid emission factors respectively. Minimum LCO_{PtG} of 194.6 €/MWh_{CH₄} was achieved, which entailed average and marginal net specific emissions of 37.2 and 635.2 gCO₂/kWh_{CH₄}, respectively. In the investigated conditions, the optimised PtG configuration produced heat in excess, but could not fulfil oxygen demand at the wastewater treatment plant. Heat integration yielded considerable performance improvements, while oxygen integration provided only minor benefits and slightly increased overall production costs. However, improved

* Corresponding author.

E-mail address: linus.engstam@slu.se (L. Engstam).

<https://doi.org/10.1016/j.apenergy.2024.124534>

Received 27 May 2024; Received in revised form 30 August 2024; Accepted 16 September 2024

Available online 21 September 2024

0306-2619/© 2024 The Author(s). Published by Elsevier Ltd. This is an open access article under the CC BY license (<http://creativecommons.org/licenses/by/4.0/>).

economic performance of oxygen integration was shown to be possible depending on local conditions. Although integrating several independent systems introduced the challenge of managing fluctuating heat and oxygen demand, alongside the varying supply of biogas and renewable electricity, the difference in magnitude between by-product generation and demand meant that their utilisation had only a minor impact on system operation.

Nomenclature		Symbols	
<i>Abbreviations</i>		ΔH	Heat of reaction [–]
CAPEX	Capital expenditure	ε	Emission factor [gCO ₂ /kWh]
CH ₄	Methane	η	Efficiency [%]
CO ₂	Carbon dioxide	κ	Ratio of specific heats [–]
DF	Demand fulfilment	λ	Usable heat fraction [%]
EF	Emission factor	C	Cost [€]
GHG	Greenhouse gas	c_p	Specific heat at constant pressure [J/(kg*K)]
H ₂	Hydrogen	E	Energy [MWh]
HHV	Higher heating value	f	Scaling factor [–]
KPI	Key performance indicator	I	Income [€]
LCOE	Levelised cost of energy	LT	Lifetime [years]
LCOM	Levelised cost of methane	n	Number of reinvestments [–]
LCOPtG	Levelised cost of power-to-gas	\dot{n}	Molar flow [mol/h]
LHV	Lower heating value	P	Electrical power [kW]
NPV	Net present value	\dot{Q}	Heat power [kW]
NSE	Net specific emissions	R	Universal gas constant [J/(mol*K)]
O ₂	Oxygen	$ReInv$	Reinvestment cost [€]
OPEX	Operating expenditure	r	Discount rate [%]
PtG	Power-to-gas	S	Scale [MW]
PEM	Proton exchange membrane	T	Temperature [K]
PV	Photovoltaics	t	Hour
RES	Renewable energy sources	x	Molar fraction [–]
SM	Supplementary material	y	Year
UF	Utilisation factor	y_i	Year of reinvestment
WWTP	Wastewater treatment plant		

1. Introduction

Reaching climate neutrality by 2050, a European Union (EU) target [1] and a necessary step to limit global warming to 1.5 °C according to the IPCC [2], will require unprecedented measures to reduce greenhouse gas (GHG) emissions, with additional deployment of renewable energy sources (RES) playing a pivotal role. In sectors where direct use of electricity from RES is either difficult or impossible, e.g. steelmaking, chemical industry, long-haul transportation and seasonal energy storage, a combination of strategies based on carbon capture, utilisation and storage may be required [3]. In regions with suitable renewable energy conditions, the concept of producing synthetic methane (CH₄) from electrolytic hydrogen (H₂) and sustainably sourced carbon dioxide (CO₂) from biogas plants through the process of power-to-gas (PtG) could be developed increase the methane yield of biogas plants [4]. Raw biogas contains 30–50 % CO₂ [5], reducing the cost of extraction [3], and the biogenic origin of the carbon means that upstream fossil emissions are significantly reduced. Thus, a completely renewable fuel capable of significantly reducing emissions could be produced [4].

This concept could accelerate defossilisation of key hard-to-abate sectors requiring an energy-dense carbonaceous fuel, as well as those needing CH₄, H₂ and CO₂ as feedstocks, since it could use existing infrastructure for transport, storage and final use. In addition, for large-scale centralised end-users, biogenic CO₂ could be recaptured for permanent storage, generating negative emissions similarly to those obtained using the bioenergy with carbon capture and storage concept [3]. PtG could also help reduce power system emissions by providing flexible

demand while allowing existing methane infrastructure to act as long-term energy storage, aiding integration of intermittent RES [6]. Through this integration of electricity and gas, and consequently various energy consumption sectors such as heat, mobility and industry, PtG would enable sector coupling, which could improve the overall efficiency of increasingly renewable energy systems [7].

Conversion of H₂ and CO₂ from biogas into synthetic methane, i.e. biogas methanation, can be done either in-situ or ex-situ. In-situ methanation involves directly injecting hydrogen into the biogas digester, enabling reduced investment costs but also risking process instability, while ex-situ methanation takes place in a separate reactor and thus offers a more stable solution, but at higher cost [8]. Ex-situ methanation of biogas can be done either directly, using raw biogas, or indirectly, using the residual CO₂ produced when biogas is upgraded to pure biomethane for vehicle use or grid injection. Since methanation of raw biogas produces biomethane with low CO₂ and H₂ content, this technology could replace conventional biogas upgrading. However, there are some technical challenges, such as varying gas composition and impurities [5,9] and a requirement for a continuous hydrogen supply to ensure a stable upgrading process [10]. The latter may inhibit the electrolyser's capability for flexible operation to enable system operators to minimise electricity costs on the spot market or match intermittent RES generation to aid local power systems. To prevent this, gas storage technologies could be used to decouple the electrolysis and methanation processes and increase flexibility [11]. Vo et al. [9] compared conventional biogas upgrading via amine scrubbing to direct and indirect methanation and concluded that although the methanation route led to significantly higher methane prices, low electricity prices

could reduce the difference, while Collet et al. [12] demonstrated that methanation could outperform conventional upgrading at electricity prices below around 40 €/MWh due to the increased methane production. Furthermore, Zhang et al. [4] emphasised the need of using low-carbon electricity to keep emissions at levels comparable to those of conventional upgrading.

As an alternative to thermochemical methanation, which requires high temperatures and pressures, biological methanation has been proposed as a suitable technology for direct ex-situ methanation of biogas. This is due to its tolerance to common biogas impurities, moderate operating conditions and high flexibility [5], and because digestate or reject water from biogas production can provide essential nutrients to the methanogenic microbes used as catalysts [13]. Nonetheless, Gantenbein et al. [14] demonstrated that biological methanation of biogas may still be more costly than thermochemical methanation, but the difference may be reduced if nutrients are supplied through digestate or reject water and the impact of intermittent operation was not considered. Due to its need for large reactor volumes, biological methanation becomes more expensive at large scales and should primarily be considered for smaller projects [15].

To increase efficiency and achieve additional economic and environmental benefits, process by-products, i.e. heat and oxygen (O₂) from electrolysis and heat from methanation, can be utilised [16–18]. Although these currently have large potential markets and high value, in district heating (DH) networks and industrial oxygen use, respectively [18,19], these markets may become saturated upon large-scale deployment of PtG and more local by-product utilisation could therefore become increasingly important. Spatially close by-product integration could also reduce handling costs and losses [19,20]. One promising option is locating PtG adjacent to wastewater treatment plants (WWTPs). On their own, WWTPs offer ample opportunities for sector coupling, as they are substantial and potentially flexible electricity and heat consumers and biogas producers, but PtG integration could provide additional benefits for both systems [21,22]. Electrolytic oxygen could reduce WWTP energy demand by replacing air in conventional aeration of the activated sludge process, which typically represents 50–70 % of electricity consumption [21,23]. Excess heat produced by electrolysis and methanation could be used e.g. to maintain sludge digester temperature. Since they are present in most urban areas, WWTPs provide a readily available by-product valorisation opportunity [22].

The concept of integrating PtG and WWTPs has been frequently explored in the literature. O'Shea et al. [24] assessed the suitability of CO₂ utilisation for PtG from different facilities in Ireland and found that WWTPs were among the most promising sources due to their high concentration of biogenic CO₂ and proximity to both gas and electricity grids. Rusmanis et al. [23,25] concluded that significant emission reductions could be achieved with an appropriately sized PtG system through additional methane production and wastewater aeration energy savings. Michailos et al. [18,26] investigated PtG as a biogas upgrading technology at a WWTP and showed that heat and oxygen utilisation could significantly improve the economic performance of the system if sold at sufficiently high prices, while Csedó et al. [27] analysed the potential of PtG at WWTPs as an energy storage technology and underlined the importance of economic performance and mentioned how limitations in by-product demand can influence this.

However, these studies considered neither temporal variations in by-product demand, nor the additional cost that come with by-product integration, both of which could have significant effect on the technical and economic performance of the integrated system. Donald and Love [28] used hourly process data to investigate shifting the energy demand at a WWTP using electrolytic oxygen and proposed introducing oxygen storage to handle supply and demand variations, while Campana et al. [21] optimised a renewable energy system including hydrogen production and both heat and oxygen utilisation at a WWTP using hourly demand data but did not elaborate on the impact of variable by-product demand. Hönig et al. [29] and van der Roest et al. [17]

considered by-product investment costs in their analyses of electrolytic oxygen and heat utilisation, respectively, and showed that these costs may influence the overall feasibility of by-product integration. However, none of these studies included methanation, which could provide additional integration opportunities.

In this study, we considered an integrated PtG system incorporating wastewater treatment with biogas production from sewage sludge, and additional biogas production through co-digestion of organic waste. The system could act as a replacement for conventional biogas upgrading, while providing further opportunities for sector coupling through local by-product utilisation. Addition of a dedicated co-digestion plant would increase the CO₂ supply, potentially reducing the discrepancy between the higher oxygen demand and lower CO₂ availability previously reported for PtG systems based on wastewater treatment [23]. We used hourly operational data from a WWTP, a co-digestion plant and renewable generation to account for temporal variations in biogas production, by-product demand and electricity supply, and analyse potential supply and demand mismatches. To our knowledge, combining all three systems is a novel approach, which was further developed by the inclusion of hourly data and by-product integration costs. The aim of the study was to provide a detailed assessment of the technical performance, economic feasibility and climate impact of the integrated system, while accounting for the effects of operational variations between the different systems integrated. Specific objectives were to:

- I. Optimise the configuration and electricity supply of a PtG system integrated with co-digestion and wastewater treatment based on hourly operational data.
- II. Quantify the techno-economic performance through evaluation of levelised cost of PtG, net specific operational GHG emissions and net energy efficiency.
- III. Analyse the implications of variable CO₂ availability and by-product demand for operation of a PtG system.

2. Methodology

2.1. System description

To enable analysis of the concept, a model of the integrated PtG system was developed. The model simulated one year of operation on an hourly basis using price and CO₂ emissions data from 2021, and hourly operational data from both the WWTP and the co-digestion plant. The PtG system analysed consisted of a PEM electrolyser and a compressed gas tank for hydrogen production and storage, and a biogas compressor and biological methanation reactor for conversion of hydrogen and CO₂ into methane (Fig. 1). The by-products, oxygen and heat, were utilised to reduce energy consumption within the WWTP, while electricity was obtained from the grid or directly from intermittent RES. Depending on the size of the system, the biogas flow could exceed the PtG upgrading capacity. Since no biogas storage was considered, any non-upgraded biogas was assumed to be flared, to ensure a high-purity output gas. The anaerobic digestion process was not included in the model, biogas production was instead represented simply through an outlet gas flow.

The PtG system was assumed to be located at a co-digestion plant in Uppsala, Sweden, where biogas from both co-digestion and sludge digestion is currently upgraded. The WWTP, located approximately 1 km from the co-digestion plant, has a population equivalence of almost 200,000 and treats approximately 20 million m³ wastewater annually. In total, the two facilities produce 60 GWh of biogas per year. The WWTP was assumed to consume 12 GWh of energy annually, of which 4.5 GWh was heat and 2.1 GWh was electricity for aeration. Heat was originally sourced from the local DH network and electricity from the electricity grid.

2.1.1. Electricity supply

Electricity could be supplied using the grid, onshore wind power

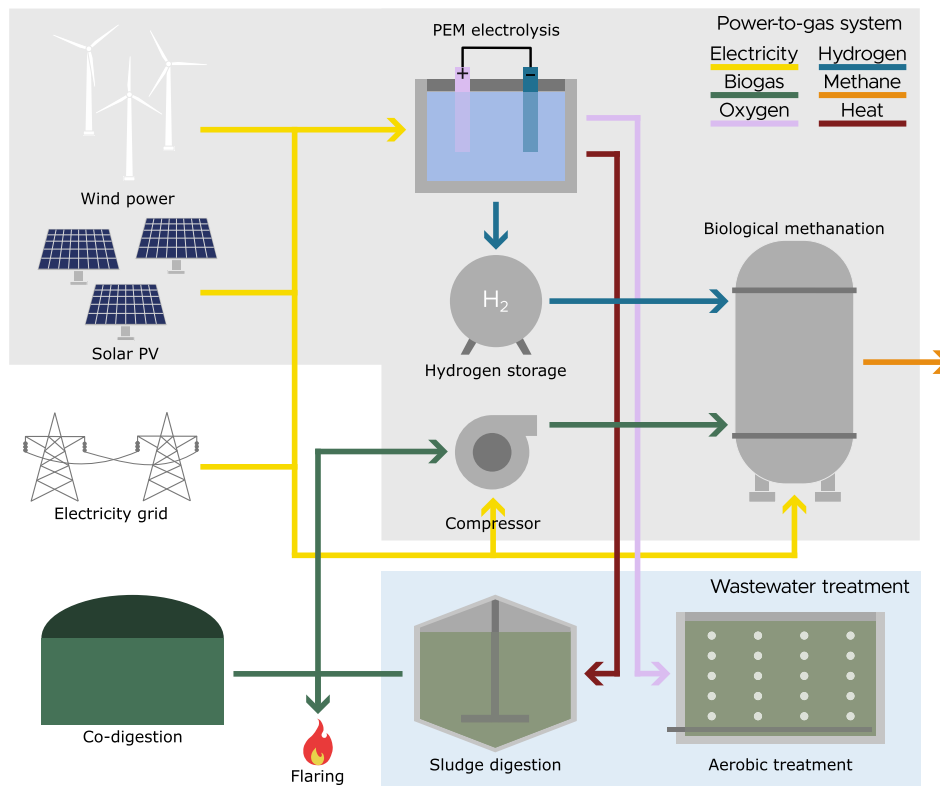


Fig. 1. Schematic overview of the integrated power-to-gas system.

through an hourly-matching power purchase agreement or on-site solar photovoltaics (PV) generation. Only PV was assumed on-site due to its suitability for deployment in urban areas, as well as actual plans for PV generation at the location. Grid electricity was purchased on the hourly spot market in SE3, one of four Swedish electricity bidding zones. Hourly purchases were assumed to entail emissions represented by hourly emission factors (EFs) for SE3 determined in a previous publication by our research group [46]. These EFs include both average emissions, i.e. grid-mix, and short-run marginal emissions, i.e. emissions associated with a slight change in demand in the current power system, and consider electricity imports and exports within the interconnected northern European electricity system and life cycle emissions for all generation technologies. Wind and PV generation were based upon hourly generation profiles in Uppsala obtained from *renewables.ninja* [60,61], average capacity factors for new onshore wind farms and utility-scale PV in Sweden [62] and annual cell degradation for PV (Table 1). Wind and PV costs were assumed to be 40 and 45 €/MWh, respectively based on levelised cost of energy (LCOE) values (Table S1). A grid fee of 10 €/MWh was assumed for grid electricity and electricity via power purchase agreement (wind), but not for local PV. Electricity taxes were not considered. To account for the uncertain value of unused RES generation during peak hours and the limited capacity of the local grid to accommodate peak generation, and thus avoid excessive RES oversizing, the impact of an excess RES generation cost equal to the production cost was also included.

2.1.2. Electrolysis

A proton exchange membrane (PEM) electrolyser was chosen due to its high flexibility capabilities. It converts liquid water (H_2O) into hydrogen and oxygen gas through endothermic electro-chemical reactions (Eqs. 1–3) and generates heat through efficiency losses due to thermodynamic irreversibilities [30].



Depending on the research objective, electrolysers can be modelled with varying degree of detail. According to Baumhof et al. [63], simpler models assuming constant efficiency or no operational states can improve runtimes, but more comprehensive representation is preferable for operational problems, especially those involving part-load operation [63,64]. Considering part-load efficiencies may also reduce operational costs [64] and provide additional information regarding excess heat generation which varies with stack efficiency [17]. In the present study, which targeted both operation analysis and optimisation, the PEM electrolyser was modelled using a linearised steady-state efficiency curve, three operational states and a thermal model.

A stack efficiency curve from Ginsberg et al. [33] was linearised in 10 segments, adapted to an assumed initial full-load stack efficiency and subjected to degradation at a rate of 1 %-unit per year (Table 1). Stack degradation reduces hydrogen production efficiency, but at the same time increases the theoretical heat recovery potential of the stack which, if this heat is utilised, could decrease the overall system efficiency loss [17]. Electrolyser system efficiency, i.e. actual electricity to hydrogen efficiency, was slightly lower than stack efficiency, due to assumed constant auxiliary energy consumption.

Despite its flexible characteristics, PEM electrolysis still experiences some operational constraints, which were modelled using three operational states: on, off or standby. When starting from cold conditions (off), start-up and heat-up times during which no hydrogen or heat, respectively, was produced were assumed. To avoid these cold start-up penalties, the option of standby was included at a cost of 2 % of nominal power. No ramping restrictions were considered, since load changes can take place within seconds [30].

Table 1
Technical parameters and assumed values for the integrated power-to-gas system.

Parameters	Used value	Unit	Literature range	Source
PEM electrolyser				
Operating temperature	80	°C	50–80	[17,30]
Hydrogen pressure	30	bar	20–70	[30,31]
Initial ^a stack efficiency	80	% _{HHV}	71–84	[30,32–34]
Initial ^a system efficiency	75	% _{HHV}	54–77	[30,32,35,36]
Minimum load	6.25 ^b	%	0–10	[11,30,32,34]
Stack lifetime	10 years ^c	hours	60,000–100,000	[30,37,38]
Degradation rate	1	%/year	0.5–2.5	[17,30,33]
Cold start-up time	5 ^d	minutes	0.2–10	[11,15,30]
Standby consumption	2	% _{of rated power}	1–5	[17,30,39]
Water consumption	0.01	m ³ H ₂ O/kgH ₂	10	[18,34]
Hydrogen storage				
Storage pressure	30	bar	30–300	[11,38,40]
Biological methanation				
Operating temperature	65	°C	60–65	[10,41,42]
Operating pressure	10	bar	5–10	[10,18,41]
Minimum load	0	%	0–10	[15]
CO ₂ conversion efficiency	99	%	98.6–100	[8,10,42–44]
Electricity consumption	0.5	kWh/Nm ³ CH ₄	0.4–0.8 ^e	[10,42,43]
Compressor				
Isentropic efficiency	75	%	75	[10,37,45]
Mechanical efficiency	95	%	95	[37,45]
Energy and emissions				
Grid emissions	Using hourly emission factors from our previous work [46]			
Wind emissions	15	gCO ₂ eq/kWh	15–16	[47–49]
PV emissions	70	gCO ₂ eq/kWh	44–112	[48–50]
PV degradation	0.5	%/year	0.5–0.6	[51]
Biogas emissions	50	gCO ₂ eq/kWh	42–122	[52,53]
DH average emissions	112	gCO ₂ eq/kWh	112	[54]
DH marginal emissions	30 ^f	gCO ₂ eq/kWh	No data	Assumption
By-products				
Usable heat fraction	80	%	80–92	[16,17,42,55,56]
Aeration energy demand	0.06 ^g	kWh/kgO ₂	0.05–0.6	[20,57–59]

^a Referring to the efficiency before stack degradation is considered.

^b Economic limit, based on assumed auxiliary energy consumption, see S2.2 in SM.

^c Converted to years, assuming 8000 h of operation per year and stack lifetime of 80,000 h.

^d Modelled as a cost, see S2.2 in SM.

^e Refers to specific consumption per unit produced in the methanation reactor.

^f Assuming biomass, value estimated based on rough conversion of electricity-based factor from [49].

^g Estimation based on actual plant data.

A thermal model was developed to describe the amount of usable heat produced by the electrolyser, which was assumed to operate isothermally. Heat generation was based on the electrolyser load and stack efficiency (Eq. 4), and the energy required to heat the input water to operating temperature (Eq. 5).

$$\text{Usable electrolyser heat} = \lambda \times [P_{\text{stack}} \times (1 - \eta_{\text{stack,HHV}}) - \dot{Q}_{\text{loss}}] \quad (4)$$

$$\dot{Q}_{\text{loss}} = \dot{n}_{\text{H}_2\text{O}} \times c_{p,\text{H}_2\text{O}} \times (T_e - T_{\text{H}_2\text{O},\text{in}}) \quad (5)$$

where λ is the usable heat fraction (section 2.2.1), P_{stack} is electricity input to the electrolyser stack, $\eta_{\text{stack,HHV}}$ is electrolyser stack higher heating value (HHV) efficiency, $\dot{n}_{\text{H}_2\text{O}}$ is input molar flow of deionised water, $c_{p,\text{H}_2\text{O}}$ is specific heat capacity of water, T_e is electrolyser operating temperature, and $T_{\text{H}_2\text{O},\text{in}}$ is temperature of the input water (15 °C).

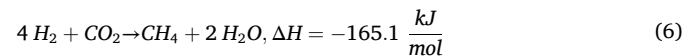
2.1.3. Hydrogen storage

To decouple electrolysis from the more continuous biogas production system and enable operational flexibility based on intermittent RES generation and spot prices (section 2.4), compressed gaseous hydrogen storage was included. A storage pressure of 30 bar was assumed, to avoid

additional compression beyond what can be achieved by the electrolyser [11]. The space requirements for low-pressure storage were assumed to be manageable for short-term stationary storage. No energy or gas losses were assumed.

2.1.4. Biological methanation

Biological methanation converts hydrogen and carbon dioxide into methane and water (Eq. 6) in a process retaining 78 %_{HHV} of the energy [15].



A continuously stirred tank reactor was assumed, represented using conversion efficiency, electricity consumption (Table 1) and a thermal model. Due to continuous biogas flow and upgrading demand, the reactor operated constantly throughout the simulations and no start-up time was necessary. Part-load characteristics were also neglected, due to lack of available information on the topic. All nutrients required were assumed to be supplied through co-digestion digestate and WWTP reject water at no additional cost, while gas polishing and recirculation was assumed to be part of the reactor system to ensure satisfactory output

gas purity. Hydrogen and CO₂ were mixed stoichiometrically.

The thermal model assumed that methanation took place in isothermal conditions. The exothermic nature of the reaction means that heat is generated upon conversion and further as water vapour condenses due to the low operating temperature and high pressure (Eq. 7) [10,65]. Depending on the temperature of the input gas, which varied based on the mixture of biogas and hydrogen, some heat was required for it to reach operating temperature (Eq. 8).

$$\text{Usable methanation heat} = \lambda \times \{ \dot{n}_{\text{CO}_2, \text{conv}} \times [\Delta H_{\text{meth}} + (2 \times x_{\text{H}_2\text{O}(l)} \times \Delta H_{\text{cond, H}_2\text{O}})] - \dot{Q}_{\text{loss}} \} \quad (7)$$

$$\dot{Q}_{\text{loss}} = \dot{n}_{\text{in}} \times \sum_i^N [x_i \times c_{p,i} \times (T_m - T_{\text{in}})] \quad (8)$$

where λ is usable heat fraction, $\dot{n}_{\text{CO}_2, \text{conv}}$ is molar flow of converted CO₂, ΔH_{meth} is heat of reaction for the methanation process, $x_{\text{H}_2\text{O}(l)}$ is fraction of liquid water in the output flow, $\Delta H_{\text{cond, H}_2\text{O}}$ is heat of condensation of water, \dot{n}_{in} is molar flow of input gases, x_i is fraction of gas i in the input gas, $c_{p,i}$ is specific heat capacity of gas i , T_m is methanation temperature, and T_{in} is temperature of the input gas.

2.1.5. Compressor

As biogas is typically produced at atmospheric pressure, compression was required for biogas to reach methanation operating pressure before injection (Fig. 1). Since the electrolyser and hydrogen storage were both operating at 30 bar, no additional compression was assumed for hydrogen. Electricity consumption by the biogas compressor was calculated as single-stage isentropic compression of ideal gas (Eq. 9).

$$P_{\text{comp}} = \frac{\kappa}{\kappa - 1} \times \frac{\dot{n}RT}{\eta_{\text{isen}} \times \eta_{\text{mech}}} \times \left[\left(\frac{p_{\text{out}}}{p_{\text{in}}} \right)^{\frac{\kappa-1}{\kappa}} - 1 \right] \quad (9)$$

where P_{comp} is required compression energy, κ is specific heat ratio (assumed to be 1.3 for biogas), \dot{n} is molar flow rate, R is the universal gas constant, T is inlet temperature, η_{isen} is isentropic efficiency, η_{mech} is mechanical efficiency, and p_{in} and p_{out} are input and output pressure, respectively.

2.1.6. Biogas production

Although the anaerobic digestion process and its operation was not included in the analysis, some techno-economic parameters in biogas production still had an impact on the performance of the PtG system. In total, the facilities produced a maximum flow of 1200 Nm³/h of biogas with a methane content of 62–65 %. About 73 % of the biogas was produced at the co-digestion plant using a thermophilic process, while the remaining 27 % was produced at the WWTP using a mesophilic process. Biogas was thus assumed to leave the digesters at 50 °C on average. Potential flaring of non-upgraded biogas due to mismatches in hydrogen production and CO₂ availability was assumed to result in additional costs and emissions from its production process. These were represented by the LCOE for biogas and its lifecycle emissions (Tables S1 and 1). Use of biogas and the CO₂ it contained was assumed to elicit no additional costs.

2.2. By-product utilisation within the integrated system

The integrated system enabled utilisation of excess heat and oxygen from the electrolyser and excess heat from the methanation reactor at the WWTP. Since the PtG system and the WWTP were 1 km apart, pipes were assumed to be used to transport both by-products. Heat and oxygen demand were modelled using a full year of hourly operational data from

a biogas plant and a WWTP situated in Uppsala, Sweden (section S2.1). By-product utilisation was limited to only the demands of the WWTP, i. e. production beyond the demand was given no value. No by-product storage was considered, so demand could only be met by production during the same hour.

2.2.1. Heat utilisation

The low-temperature nature of the excess heat generated, assumed to

be 50–60 °C [17,42], limited its potential applications to usage areas such as heating of digesters for biogas production and low-temperature DH systems [5,19]. However, since third-generation DH is currently used in Uppsala, requiring temperatures of near 100 °C, and the co-digestion plant requires above 70 °C for hygienisation and thermophilic operation, excess heat from the PtG system was assumed to be used solely at the WWTP for maintaining operating temperature in two mesophilic sludge digesters and for auxiliary low-temperature heat demands such as facility heating, avoiding the costs and emissions associated with the DH currently used.

To account for heat losses in the thermal models (Eqs. 4 and 7), the usable heat fraction (λ) was defined as the amount of actual heat possible to utilise in other applications divided by the theoretical net heat generation. A value of 80 % was chosen based on literature estimates for both electrolysis and methanation (Table 1, section S2.3 in SM). It was also assumed that no usable heat could be extracted from auxiliary components, i. e. only from the electrolyser stack and the methanation reactor.

2.2.2. Oxygen utilisation

Oxygen produced via electrolysis could be utilised to replace air for aeration in the activated sludge process in the WWTP. The higher oxygen content (100 % instead of 21 %) would lead to higher partial pressure, and consequently higher driving force [57]. This would theoretically allow for a reduction in gas flow rate and corresponding aeration energy consumption by a factor of 4.76, without loss in treatment quality [22]. Use of pure oxygen instead of air would also increase oxygen transfer rate (OTR) by increasing the mass transfer coefficient and thus further reduce aeration flow rate and associated electricity demand [57]. Although pure oxygen has been used in wastewater treatment processes for decades [23], the practice is still rare and the extent of the OTR increase remains ambiguous. Previous studies on the topic have theorised that the increase could reach 20 % using conventional equipment [57] or 300 % using aeration systems specifically made for pure oxygen [28]. However, such improvements are yet to be demonstrated in large-scale settings and may be offset by an increased need for mixing [22,57]. In this study, aeration energy savings were initially attributed solely to the reduced flow rate, i. e. a reduction factor of 4.76, and additional effects were neglected. The aeration energy requirement was estimated at 0.06 kWh/kgO₂ using operational data (Table 1), which was in the lower range of literature values since consumption data were only available for the most recently constructed part of the plant, finalised in the 2010s.

Based on conversations with the WWTP operator and literature [29,58], pure oxygen was assumed to be supplied through a separate, parallel aeration system. The pure oxygen system could be used to completely or partly meet the oxygen demand and reduce aeration energy consumption proportionally to the replaced air [22,23]. No oxygen compression was deemed necessary, since the electrolyser can deliver oxygen at the required pressure level, and oxygen purity of 100 % was assumed [28,29]. The same electricity price was assumed for aeration at

the WWTP as for hydrogen production, i.e. hourly spot prices.

2.3. Techno-economic assessment

To analyse the characteristics of the integrated PtG system, techno-economic and environmental assessment methods were used and key performance indicators (KPIs) defined. Due to high inflation rates, significant cost increases have been seen in recent years, in particular for electrolyzers, which have also seen material and labour cost increases [66]. Because of this, all economic parameters were converted to €₂₀₂₃ based on the reference year of the data, or the year before publication year if no reference year was provided. A detailed overview of the economic parameter values can be found in Table S1. Moreover, all efficiency and energy values were defined based on the HHV [17].

Economic performance was primarily evaluated using levelised cost of power-to-gas (LCOPTG), an extension of LCOE also incorporating the avoided costs from by-product utilisation, as previously done in [67], signifying the potential gas value at which system expenses and revenues are equal (Eq. 10). We also included the cost of flared biogas within the LCOPTG, defined using LCOE for biogas, to penalise the additional gas flaring caused by PtG systems smaller than the maximum biogas flow. This indicator considered only the costs associated with the PtG system and the synthetic methane it produces, and not the overall cost of methane production from the facility. To evaluate the overall methane production cost, and simplify comparison with other systems, the levelised cost of methane (LCOM; Eq. 11) was introduced. LCOM is a further expansion of LCOPTG, where the total biomethane produced through anaerobic digestion and its costs are included. Hereafter, synthetic methane refers to methane produced by the PtG system, while biomethane refers to the methane already present in the biogas. Economic performance was also evaluated using the net present value (NPV; Eq. 12), representing the current value of all cash flows, including discounted future costs and income. A positive value indicates a profitable investment and a negative value an unprofitable investment.

$$LCOPTG = \frac{CAPEX + \sum_{y=1}^{LT} \left[\frac{OPEX + (LCOE_{bg} \times E_{bg,flared}) - I_{bp}}{(1+r)^y} \right] + \sum_i^n \left[\frac{ReInv_i}{(1+r)^{y_i}} \right]}{\sum_{y=1}^{LT} \left[\frac{E_{CH_4,PtG}}{(1+r)^y} \right]} \quad (10)$$

$$LCOM = \frac{CAPEX + \sum_{y=1}^{LT} \left[\frac{OPEX + (LCOE_{bg} \times E_{bg,tot}) - I_{bp}}{(1+r)^y} \right] + \sum_i^n \left[\frac{ReInv_i}{(1+r)^{y_i}} \right]}{\sum_{y=1}^{LT} \left[\frac{E_{CH_4,tot}}{(1+r)^y} \right]} \quad (11)$$

$$NPV = \sum_{y=1}^{LT} \frac{I - OPEX}{(1+r)^y} - CAPEX \quad (12)$$

where CAPEX is capital expenditure of the system, OPEX is annual

operating expenditure consisting of a fixed and variable part (electricity and water costs), $E_{CH_4,PtG}$ and $E_{CH_4,tot}$ are annual methane production by the PtG and total methane production, respectively, $E_{bg,flared}$ and $E_{bg,tot}$ are annual biogas flaring and total biogas production, respectively, $LCOE_{bg}$ is levelised cost of energy for biogas, I is income or avoided cost from by-product utilisation, y is year, $ReInv_i$ represents reinvestments taking place in specific years during project lifetime such as electrolyser stack replacements, y_i is year of reinvestment i , n is number of reinvestments during the project lifetime, LT is system lifetime, and r is discount rate. The variable OPEX constituted electricity, water, standby and start-up costs.

The specific CAPEX of some of the main components included in the PtG system have been demonstrated to undergo scaling effects, i.e. decrease with increasing nominal capacity. To account for the varying component sizes investigated in this study and their impact on economic performance, these scaling effects were described using the relationship defined in Eq. 13 [67].

$$C_b = C_a \times \left(\frac{S_b}{S_a} \right)^f \quad (13)$$

where S_a is reference scale, S_b is desired scale, C_a is reference cost, C_b is cost at the desired scale, and f is scaling factor. All assumed reference values and scaling factors can be found in Table 2. See section S2.4 in SM for a detailed account of the literature and cost estimation methodology.

Technical aspects such as system efficiency and by-product utilisation fractions were defined to describe system operation and performance. System efficiency was indicated by net energy efficiency (η_{net}), defined as energy content of the output gas and energy avoided from by-product utilisation, divided by total input electricity (Eq. 14).

$$\eta_{net} = \frac{E_{CH_4,PtG} + E_{heating} + E_{aeration}}{E_{PEM} + E_{meth} + E_{comp}} \quad (14)$$

where E_{PEM} , E_{meth} and E_{comp} are electricity consumption in electrolysis, methanation and compression, respectively, and $E_{heating}$ and $E_{aeration}$ are avoided energy consumption from heat and oxygen utilisation, respectively.

By-product utilisation was investigated from both production and demand perspectives. From a production perspective, heat and oxygen utilisation factors were defined (UF_{heat} and UF_{O_2}) according to Eq. 15. From a demand perspective, demand fulfilment (DF_{heat} and DF_{O_2}) was instead defined by Eq. 16.

$$UF = \frac{\text{Utilised amount}}{\text{Annual production}} \quad (15)$$

$$DF = \frac{\text{Utilised amount}}{\text{Annual demand}} \quad (16)$$

In addition, the climate impact was quantified using net specific emissions (NSE), which included avoided emissions from by-product utilisation and emissions from flared biogas (Eq. 17). These were

Table 2

Scaling factors and reference values used for capital expenditure (CAPEX) determination.

Component	Reference cost ^a	Reference scale	Scaling factor	References
PEM electrolyser	1500 ^b €/kW _{el}	5 MW _{el}	0.75	[33,39], [67–69]
Biological methanation	900 €/kW _{CH₄}	5 MW _{CH₄}	0.65	[18,39,42,67]
Compressor	30,000 €/kW _{el}	1 kW _{el}	0.48	[45]
Hydrogen storage	500 €/kgH ₂	–	1	[11,21,38,70]
Oxygen piping	540 €/m	–	1	[17,71]
Pure oxygen aerator	70 €/kW _{electrolyser}	1.25 MW _{el}	0.6	[29,67]
Heat piping	230 €/m	–	1	[17]
Heat extraction	260 €/kW _{th} ^c	400 kW _{th}	0.3	[17]

^a Refers to non-installed cost, converted to €₂₀₂₃.

^b Assuming a value in the higher range of literature values to further account for recent cost increases.

^c Refers to usable heat generation from both electrolyser and methanation.

defined using both average and marginal emission data for electricity and DH. Only operational emissions were considered, i.e. emissions from manufacturing and emission reductions from fossil fuel replacement were disregarded.

$$\text{Net specific emissions} = \frac{\sum_{t=1}^N \{ [(P_{g,t} - P_{a,t}) \times \varepsilon_{g,t}] + (P_{w,t} \times \varepsilon_w) + (P_{pv,t} \times \varepsilon_{pv}) - (P_{dh,t} \times \varepsilon_{dh}) \} + (E_{CH_4,flared} \times \varepsilon_{bg})}{E_{CH_4,PtG}} \quad (17)$$

where $P_{g,t}$ is grid electricity use at hour t , $P_{w,t}$ is wind electricity use at hour t , $P_{pv,t}$ is solar PV electricity use at hour t , $P_{dh,t}$ is replaced DH at hour t , $P_{a,t}$ is replaced aeration energy at hour t , $\varepsilon_{g,t}$ is grid EF at hour t , ε_w is wind EF, ε_{pv} is solar PV EF, $\varepsilon_{dh,t}$ is DH EF at hour t , ε_{bg} is biogas EF, and N is number of hours in a year.

2.4. Operating strategy

Electrolyser dispatch was determined using an operating strategy based on mixed-integer linear programming (MILP), which has previously been adopted for electrolyser dispatch problems [63,72]. We defined a three-state model in which the electrolyser could be in on, off or standby mode based on the model proposed in [63]. While the advantages of a three-state model may be reduced by the quick start-up capabilities of PEM electrolysis, addition of a heat-up period increases the format's usefulness when addressing high-resolution heat utilisation. Limited foresight of 24 h was applied to more closely represent actual system operation using intermittent RES and hourly spot prices [73,74], meaning that operation was optimised on a daily basis. However, perfect foresight for RES generation, spot prices and biogas and WWTP operation was assumed within the 24-h period, which may lead to a slight underestimation of the overall operational costs as shown in [74].

The objective function aimed to minimise operational costs over an upcoming 24-h period considering the cost of electricity, standby and start-up costs, and avoided costs from by-product use. The latter meaning avoided electricity and heat purchases due to reduced energy consumption at the WWTP. Electrolyser operation was constrained by its load range, storage capacity and an hourly hydrogen demand, based on CO₂ availability. Hydrogen production was determined via the piecewise linearised efficiency curve described in section 2.1.2, meaning that part-load efficiency variations were included. Electricity could be acquired on the day-ahead spot market or directly from RES generation. RES generation was assumed to entail no cost within the operating strategy, to prioritise its use. Using hourly profiles for grid electricity price, RES generation and heat and oxygen demand, and seasonal DH prices, the cost-optimal electrolyser dispatch was determined. Excess hydrogen production could be stored and used to fulfil demand at a later time. End-of-day values for electrolyser and storage states were used as constraints for optimisation of the following day. Since methanation and biogas compression operated solely based on CO₂ availability and were assumed to be fully flexible, they were not included in the operating strategy. A detailed formulation of the operating strategy can be found in section S4 in SM.

Table 3

Nominal capacity ranges and step sizes investigated for all optimisation parameters.

Plant parameter	Capacity range	Step size	Unit
Electrolyser	6–12	0.5	MW _{el}
Methanation reactor	3.5–5	0.5	MW _{CH4}
Hydrogen storage	0–1000	100	kgH ₂
Oversizing factor	0–3	0.5	RES to electrolyser
PV fraction	0–100	25	% of RES

2.5. Configuration optimisation methodology

Component sizes and electricity supply were optimised in parallel with system operation to obtain the minimum production cost. PtG

system components (electrolyser, hydrogen storage and methanation reactor) were sized in relation to CO₂ availability, with the objective of minimising LCOPtG. The inclusion of biogas flaring costs in the LCOPtG indicator meant that the trade-off between lower CAPEX and increased flaring that occurs for smaller PtG systems was considered in the optimisation. A rather narrow solution space was defined through manual investigation, to reduce computational costs (Table 3). The methanation reactor capacity range was set by the peak biogas production (5 MW_{CH4}), potentially reducing biogas flaring to zero, and the smallest electrolyser capacity (3.5 MW_{CH4}), reducing CAPEX while necessitating some flaring. The biogas compressor was sized in relation to the methanation reactor and was thus not optimised. During the optimisation runs, the lifetime degradation of the electrolyser and solar PV was averaged into single-year values, again to shorten runtime.

Previous studies have concluded that oversizing directly coupled RES can provide economic and environmental benefits for PtG systems [46,75,76]. These effects could be enhanced if wind and solar PV were deployed in conjunction, i.e. hybridisation, due to their complementary generation profiles in the region [77,78]. To obtain the overall cost-minimising configuration for varying electricity supply mixes, configuration optimisation was conducted for different RES oversizing factors and different mixes of wind and PV generation (Table 3). As described in section 2.1.1, a cost for excess RES generation was included. If several facilities in the local energy system operate using significantly oversized RES generation, the electricity price during hours of peak generation may decrease and consequently lower the value of selling excess electricity to the grid. Thus, this cost ensures the trade-off between high RES use and local energy system balance is considered and may be seen as a conservative estimation of RES generation costs.

3. Results and discussion

3.1. Optimisation results

The PtG component and electricity supply optimisation resulted in a

Table 4

Component sizing of the cost-optimal configuration.

Plant parameter	Optimised value	Unit
Electrolyser	8.5	MW _{el}
Methanation reactor	5	MW _{CH4}
Hydrogen storage	300	kgH ₂
Oversizing factor	2.5	RES to electrolyser
PV fraction	50	% of RES

Table 5

Key performance indicator (KPI) performance of the cost-optimal configuration.

KPI	Value	Unit
LCOPtG	194.6	€/MWh _{CH4}
LCOM	112.9	€/MWh _{CH4}
η_{net}	59.7	% _{HHV}
Average NSE	37.2	gCO ₂ eq/kWh _{CH4}
Marginal NSE	635.2	gCO ₂ eq/kWh _{CH4}

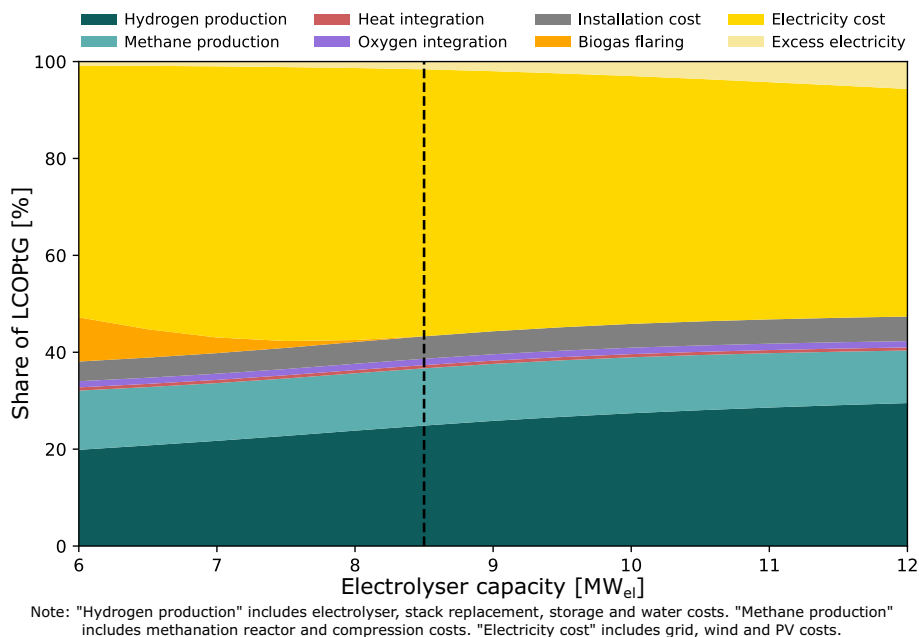


Fig. 2. Cost-breakdown for varying electrolyser capacities assuming a 5 MW_{CH₄} methanation reactor, 300 kgH₂ storage and a renewable energy source (RES) oversizing factor of 2.5 with 50 % photovoltaics (PV). The dashed line indicates optimised electrolyser capacity.

single configuration (Table 4) achieving minimum LCOPTG of 194.6 €/MWh_{CH₄} (3 €/kgCH₄) (Table 5). This system reduced biogas flaring to nearly 0 %, resulting in 95.8 GWh of total methane production, of which 35.4 GWh (37 %) was synthetic methane originating from the PtG system. Minimum LCOM, i.e. overall methane production cost including biomethane, of 112.9 €/MWh_{CH₄} was produced by the same configuration, since minimising LCOPTG also minimised LCOM due to the constant biogas production in all configurations. This represented a 74 % increase from the assumed LCOE for biogas of 65 €/MWh. The impact of raw biogas cost on LCOM is shown in Fig. S1 in SM. Net energy efficiency of 59.7 %_{HHV} (53.7 %_{LHV}) was achieved, representing conversion of electricity into methane as well as energy savings at the WWTP from by-product use, which increased to 78.7 %_{HHV} (70.9 %_{LHV}) when the whole biogas upgrading system was considered (including

biomethane). Without considering excess RES costs, LCOPTG and LCOM were reduced to 191.3 and 111.7 €/MWh_{CH₄}, respectively.

The main cost component of the PtG system was electricity, followed by the electrolyser and methanation units (Fig. 2). In the optimised case, most of the electricity (96 %) was used in the electrolysis process, meaning that hydrogen production was indirectly responsible for almost 80 % of total LCOPTG. The remaining electricity consumption was shared evenly between methanation and compression (2 % each) (Fig. S2 in SM), in line with literature values for biological methanation (2–2.5 %) [5].

The LCOPTG value was at the higher end of previous estimates for methane production through PtG, due to CAPEX increases, inflation and high electricity prices in recent years [11,26]. As these parameters are highly variable depending on year and location, their influence was

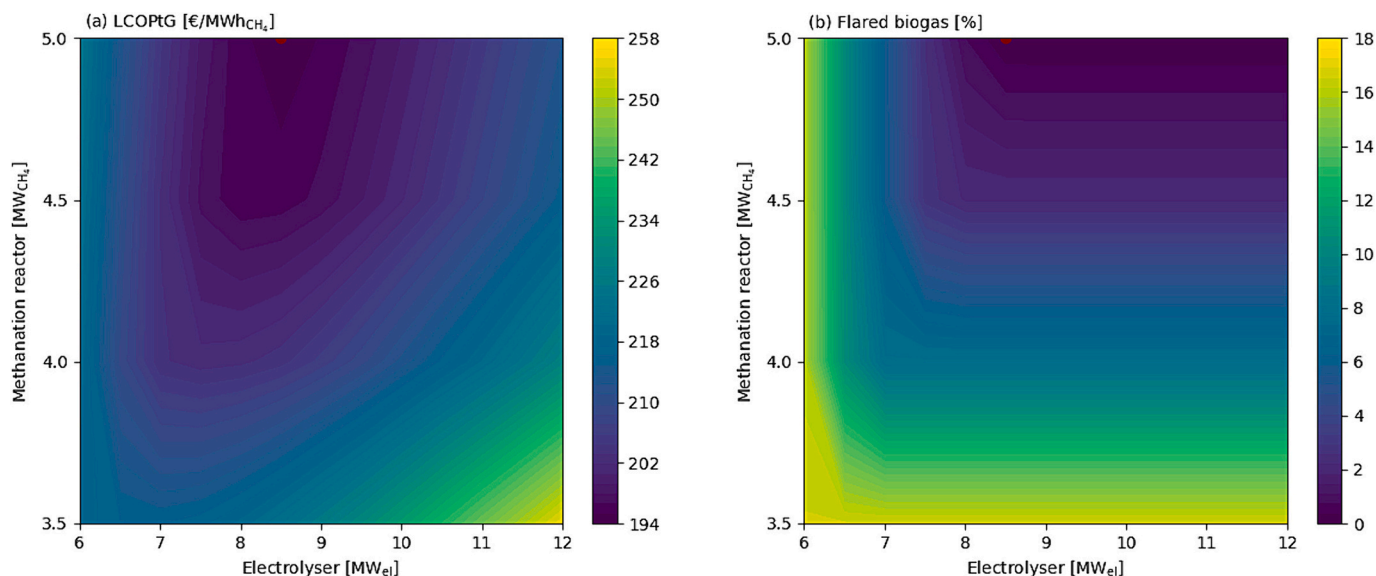


Fig. 3. Impact of electrolyser and methanation capacity on (a) levelised cost of power-to-gas (LCOPTG) and (b) flared biogas for a system with a 300 kgH₂ storage, using a renewable energy source (RES) oversizing factor of 2.5 and 50 % photovoltaics (PV). The red dot indicates minimum LCOPTG. (For interpretation of the references to colour in this figure legend, the reader is referred to the web version of this article.)

further investigated (section 3.4). Compared with the current state-of-the-art biogas upgrading technology, amine scrubbing, LCOM was 54 % higher using PtG, assuming CAPEX of 2300 €/Nm³/h for amine scrubbing (73.2 €/MWh; section S2.4 in SM). This is in line with the 32–88 % increase demonstrated for direct methanation of biogas compared to amine scrubbing by Vo et al. [9] for electricity prices between 50 and 100 €/MWh. However, the increase in methane production meant that PtG yielded higher NPV for biomethane prices above 180 €/MWh_{CH₄} (2.8 €/kgCH₄; Fig. S3 in SM).

The climate impact of the methane produced was greatly affected by the type of grid EF used, because grid electricity comprised 39 % of the electricity supply to the optimised configuration (section 3.1.2). The local electricity mix provided low-carbon electricity sourced primarily from hydro, nuclear and wind power, as net specific emissions of 37.2 gCO₂/kWh_{CH₄} were achieved using solely the 2021 average grid-mix. This corresponded to a 79 % decrease compared with fossil methane with a carbon content of 178 gCO₂/kWh_{CH₄} (HHV), exceeding the 70 % reduction target set by the EU [79]. Assuming that the additional gas produced by the PtG system is used to replace fossil methane, annual emission savings of nearly 5000 tCO₂ would be achieved using the average net specific emissions of the optimised configuration. This corresponds to a carbon abatement cost of 1378 €/tCO₂, which is considerably higher than the current EU ETS prices of 50–100 €/tCO₂ [80], but in line with previous estimates for synthetic fuels [81]. Conversely, emissions were significantly higher when considering the short-run system-wide marginal implications within the interconnected northern European power system, as net specific emissions of 635.2 gCO₂/kWh_{CH₄} were achieved using 2021 marginal EFs. This can be attributed to the predominantly fossil composition of marginal generation, and highlights the importance of using low-carbon electricity to ensure definite climate benefits of PtG systems. However, marginal emissions may be reduced in the long run as flexible demand such as PtG may increase the share of intermittent RES in the electricity mix, and the net specific marginal emissions may thus be a conservative value. Readers are referred to previous work by the authors [46] for a more detailed analysis regarding the implications of the short-run marginal EFs used in this study.

Moreover, note that this analysis only includes operational emissions from the PtG plant, which, although typically representing the majority of emissions from PtG systems [4], means that the climate impact would likely increase if a life cycle perspective was used. The impact of

methane leakage can also be significant for the overall climate impact [4]. Although this was included in the assumed biogas emissions, the leakage rate varies between sites and additional leakage could occur within the PtG system to further increase emissions. Previous studies on life cycle assessment of PtG systems provide emissions between 18 and 90 gCO₂/kWh_{CH₄} using renewable electricity and 406–828 gCO₂/kWh_{CH₄} using grid mixes consisting of both renewable and fossil generation [82,83], in line with the estimations from average and marginal perspectives respectively in this study.

3.1.1. Impact of power-to-gas component sizing on performance

Configuring the power-to-gas system to minimise biogas flaring without excessively oversizing the electrolyser, reducing investment and potentially excess RES costs, appeared to be crucial in achieving low production costs. Fig. 3 demonstrates how LCOPTG was minimised using the smallest electrolyser and methanation capacities capable of reducing biogas flaring to near 0 %. Addition of hydrogen storage enabled decoupling of electrolysis and methanation, which allowed for more electrolyser operation during hours of low spot prices or RES generation and consequently reduced LCOPTG (Fig. 4). However, due to limited oversizing of the electrolyser and fairly constant hydrogen demand, relatively short-term storage was able to minimise production costs, as 300 kgH₂ corresponds to approximately 2 h of full load operation for an 8.5 MW_{el} electrolyser. Overall, component optimisation revealed that a rather large number of configurations were able to produce LCOPTG values close to the minimum value, so the optimal configuration may perhaps be described more appropriately as a range of component values, as concluded in previous studies [11]. For example, LCOPTG was within 2 % of the minimum for 76 configurations with component size between 7.5 and 9.5 MW_{el} (electrolysis), 4.5–5 MW_{CH₄} (methanation) and 100–1000 kgH₂ (storage).

Net energy efficiency was mainly influenced by part-load operation possibilities and was thus maximised using large electrolysers (Fig. S4 in SM). Hydrogen storage, on the other hand, had a negative effect on system efficiency, since it enabled more overproduction at high loads balanced by complete shutdowns. Limited heat demand at the site (further explored in later sections) meant that net energy efficiency was maximised for small methanation reactors in combination with large electrolysers, which reduced non-utilised heat generation while still enabling part-load operation. However, any economic benefits of efficiency improvements based on these factors were counteracted by

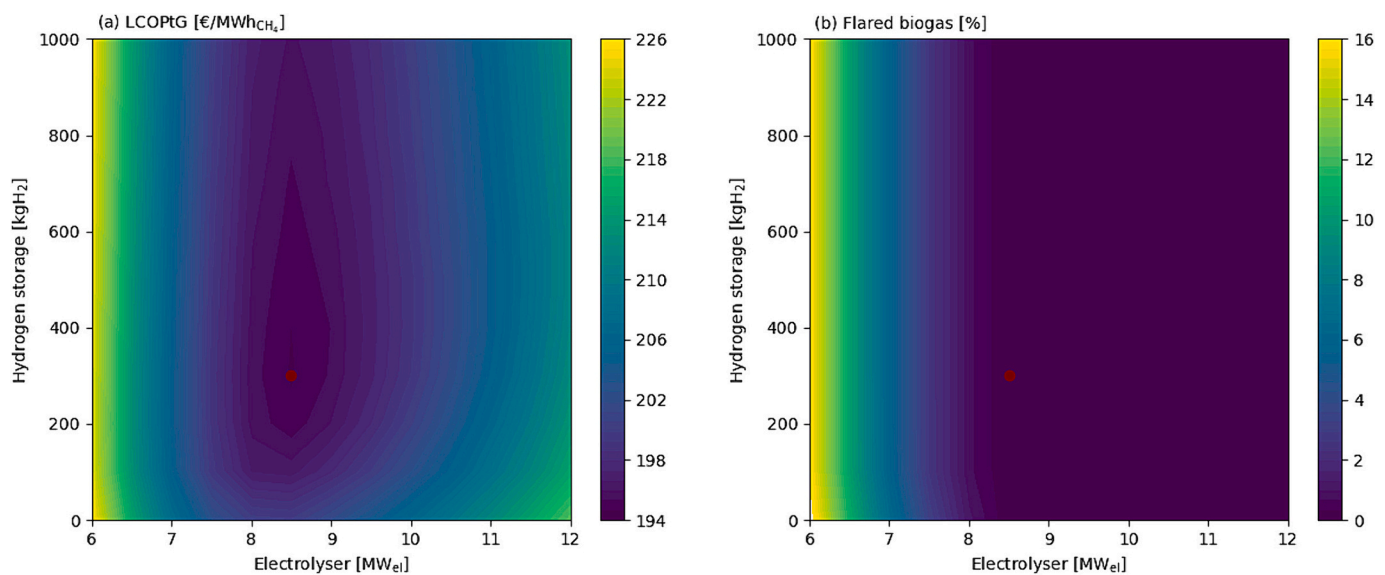


Fig. 4. Impact of electrolyser and hydrogen storage capacity on (a) levelised cost of power-to-gas (LCOPTG) and (b) flared biogas for a system with a 5 MW_{CH₄} methanation reactor, using a renewable energy source (RES) oversizing factor of 2.5 and 50 % photovoltaics (PV). The red dot indicates minimum LCOPTG. (For interpretation of the references to colour in this figure legend, the reader is referred to the web version of this article.)

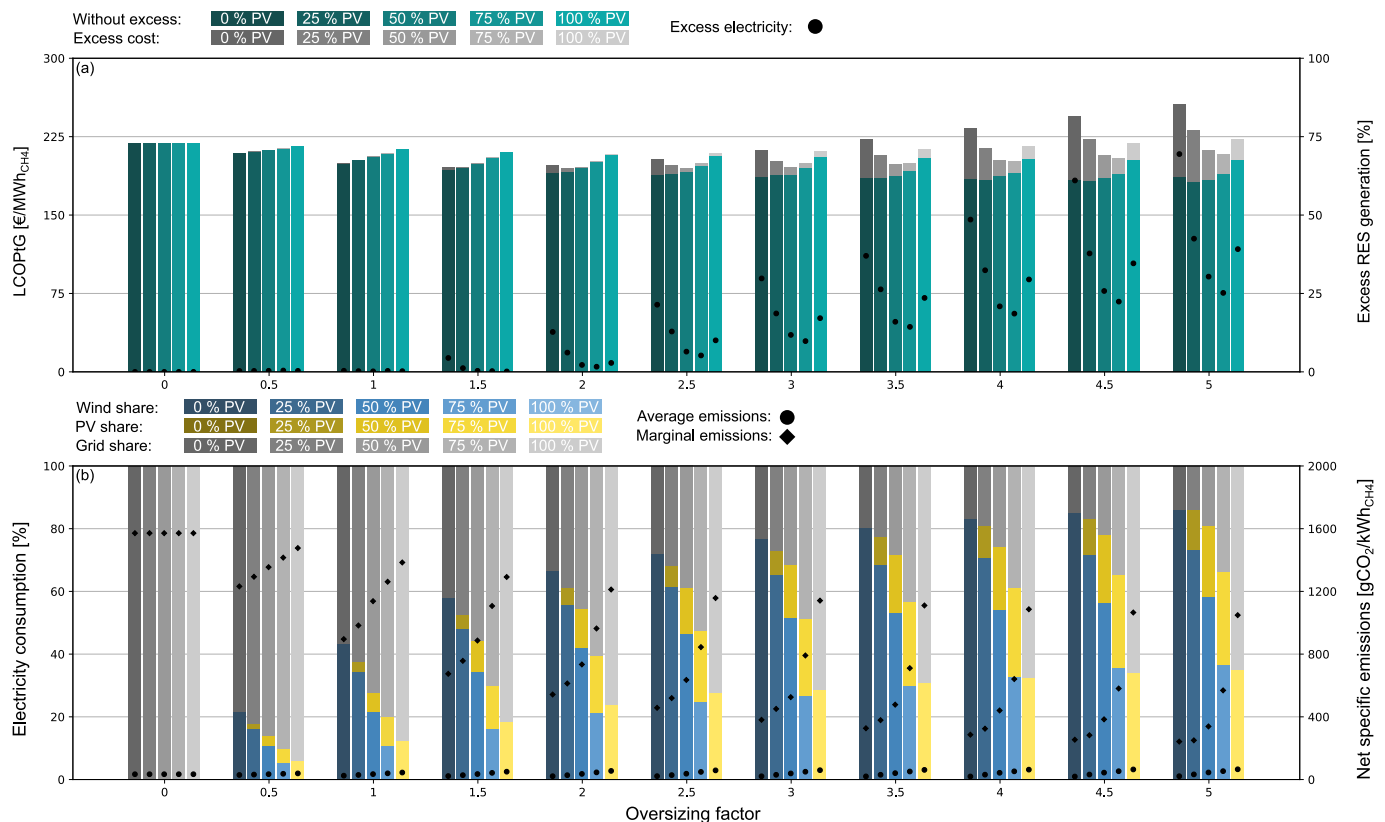


Fig. 5. Impact of renewable energy source (RES) oversizing (x-axis) and hybridisation factor (colour) on (a) minimum levelised cost of power-to-gas (LCOPtG) (bars; left) and excess RES generation (markers; right) and (b) electricity mix (bars; left) and net specific emissions (markers; right).

increased investment and flaring costs.

Similarly, more significant oversizing of the electrolyser, and thus RES generation, compared with the methanation reactor caused an increase in the fraction of directly coupled renewable electricity used in the process. This reduced marginal net specific emissions further (to a minimum of 336 gCO₂eq/kWh_{CH4} using the optimised electricity supply; Fig. S5 in SM), but came at significant economic cost (254 €/MWh_{CH4}) due to increased biogas flaring, electrolyser investment costs and excess RES generation. The impact based on average EFs was limited due to the low-carbon characteristics of the grid (Fig. S6 in SM).

3.1.2. Electricity supply analysis

Due to the lower costs assumed for RES generation compared with grid electricity, achieving high RES share through oversizing was found to have a positive impact on LCOPtG (Fig. 5a). Moreover, the complementary generation profiles of wind and solar meant that hybridisation enabled higher RES shares in the supply mix while avoiding significant excess generation. When the cost of excess renewable electricity was also included, and thus minimised, the lowest production costs were achieved by maximising the share of renewable electricity while keeping excess RES below 15 % (Fig. 5a). Consequently, the cost-optimal configuration was obtained using an oversizing factor of 2.5 with 50 % wind and 50 % solar PV (10.625 MW each for an 8.5 MW_{el} electrolyser). However, the factor and ratio values depended on the specific generation profiles and cost assumptions used, and previous studies suggest that the optimal PV fraction in the region may be closer to 25 % [77]. The realisable potential of on-site PV also depends on spatial limitations at the location. When excess RES costs were not included, LCOPtG was reduced by 1.7 % for the optimised configuration, but the minimum value (181.1 €/MWh_{CH4}; Table S3 in SM) was instead achieved using the largest possible oversizing. The impact of electricity supply and excess cost on system configuration is further analysed in

section S3.1 in SM.

Due to the mismatch between RES generation and biogas production, the inclusion of hydrogen storage could enable higher RES fractions. This was true especially for systems with a high PV fraction, where the daily variations were more distinct (Table S3). However, significant oversizing of wind power reduced the number of periods with low RES generation and thus the need for large storage capacities. Furthermore, the impact of storage on the RES fraction was limited as the possibility of grid utilisation provided an alternative means of fulfilling the hydrogen demand from biogas upgrading without resorting to excessive RES and hydrogen storage oversizing. In the optimised case, hydrogen storage enabled only a 3 %-unit increase in RES fraction.

As discussed in section 3.1, grid utilisation entailed large emissions from a short-run marginal perspective (Fig. 5b), and also meant that not all methane produced complied with the principles of production of renewable fuels of non-biological origin (RFNBOs) recently defined by the EU, i.e. temporal and spatial correlation with newly constructed RES generation [79]. Achieving full grid independence required either significant RES oversizing or increasing electrolyser and energy storage capacities, which were both accompanied by higher production costs when excess RES costs were included. However, grid operation may be possible within the RFNBO framework if the local electricity system already contains more than 90 % renewables, as is the case for northern Sweden, and could provide additional benefits to the system. The flexibility of PtG systems means that they can provide auxiliary services to the local electricity grid, such as frequency regulation. This could be a significant source of income and lead to non-negligible reductions in production cost for grid-operated systems [18,30]. Furthermore, a grid-connected system may avoid curtailment of excess RES generation through grid sales and consequently lower the excess costs and LCOPtG. Exporting electricity to the grid could also lead to avoided grid emissions and reduce the climate impact of the system.

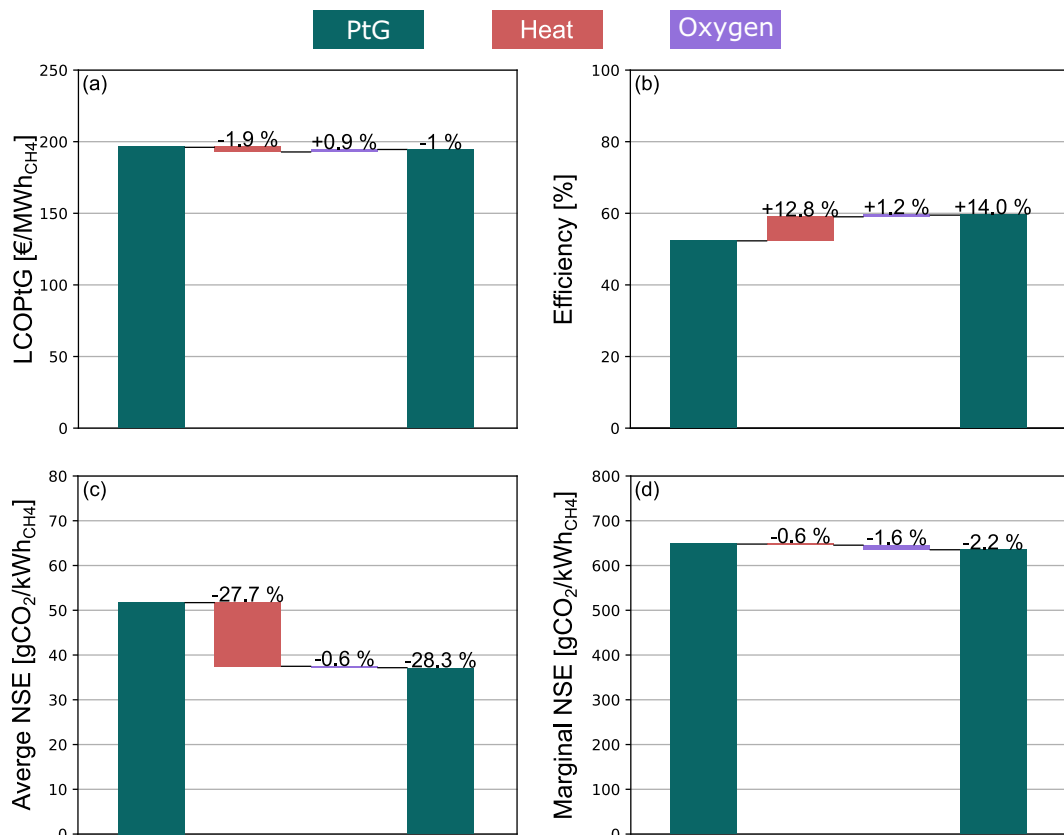


Fig. 6. Relative impact of by-product utilisation in the optimised system on (a) levelised cost of power-to-gas (LCOPtG), (b) net energy efficiency and net specific emissions (NSE) from (c) average and (d) marginal perspectives.

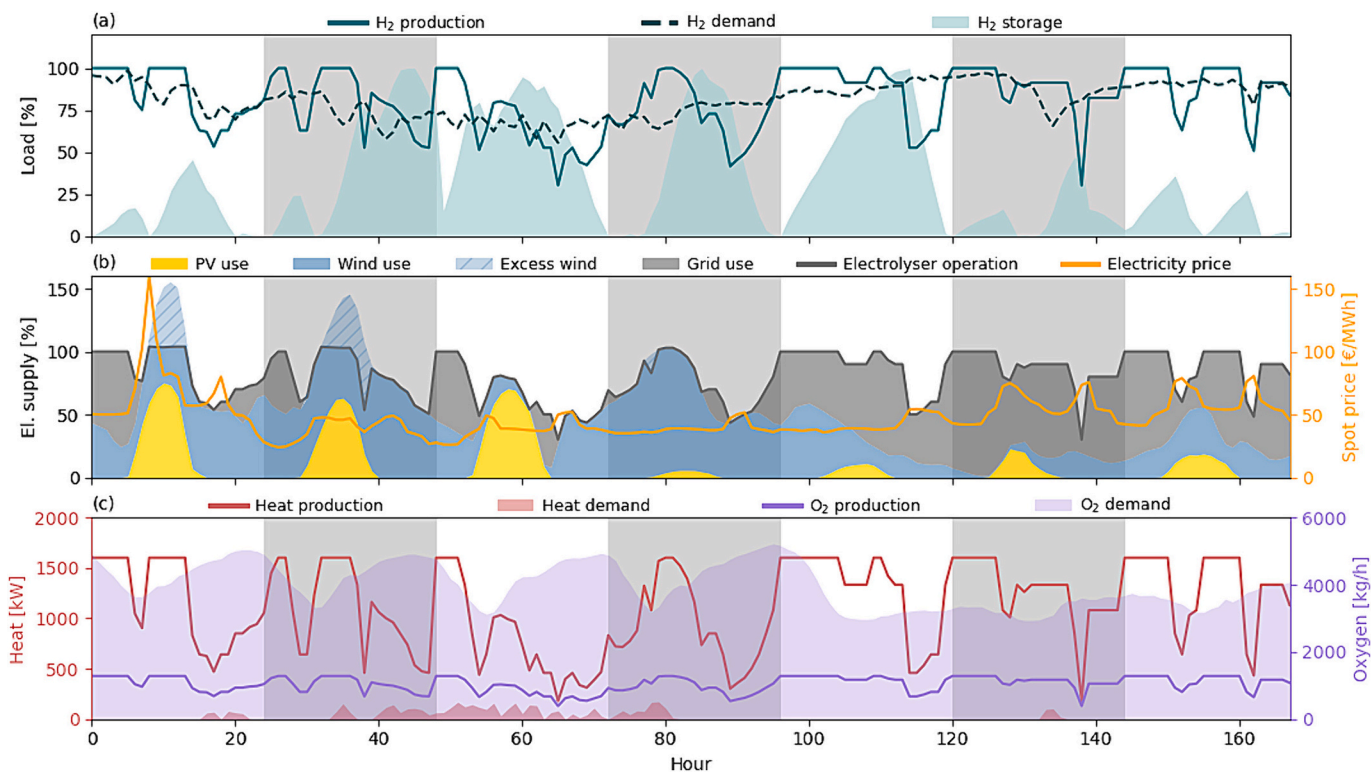


Fig. 7. One-week sample of (a) electrolyser and hydrogen storage operation, (b) electricity supply and hourly spot price and (c) by-product generation and demand. Days are separated using grey and white background. Note that the heat demand only includes what could not be met by the methanation reactor.

3.2. Impact of by-product utilisation

Our analysis highlighted both the benefits and challenges of a locally integrated PtG system. Using data from the co-digestion plant and WWTP in Uppsala, Sweden, by-product utilisation improved overall techno-economic performance by increasing net system efficiency and providing both economic and environmental benefits. In the optimised configuration, an efficiency increase of 7.4 %-units was seen when by-product utilisation was considered, while LCOPTG and average and marginal net specific emissions were reduced by 1.0, 28.3 and 2.2 %, respectively (Fig. 6). However, on considering the impacts of heat and oxygen separately, the main contribution came from heat utilisation, through which 4544 MWh (41 % of total WWTP energy consumption) were avoided, whereas the use of oxygen only led to minor efficiency and emission improvements and increased overall production costs, with 434 MWh (21 % of aeration electricity; 4 % of total energy) avoided. The exception was emissions from a marginal perspective, where the assumption of biofuels on the margin within the DH network lessened the impact of heat utilisation and the observed reduction instead originated in avoided marginal electricity from oxygen use.

Although its impact was larger than that of oxygen, heat utilisation within the integrated system was constrained by the heat demand of the WWTP. All configurations studied achieved heat demand fulfilment (DF_{heat}) of around 99.9 %, i.e. fulfilled nearly all heat demand, and a heat utilisation factor (UF_{heat}) of only 25.2 % was required using the optimised configuration, meaning the only a quarter of the heat produced was utilised. However, because of temporal mismatches between heat generation and demand, 0.1 % of the demand was not fulfilled and instead relied on DH. For smaller systems, the heat generation was smaller, leading to higher heat utilisation factor and consequently system efficiency, and vice versa. Since the higher heat utilisation system investment cost induced by a larger system was not balanced by higher avoided costs, the limited heat demand counteracted the scaling effects for heat integration, and consequently reduced NPV_{heat} and the potential LCOPTG decrease for larger systems (Fig. S7 in SM). This could be managed by sizing the heat integration components after demand

instead of production, but positive NPV_{heat} was nonetheless achieved in all system configurations (1382 k€ in the optimised case). The limited heat demand also meant that the net energy efficiency decrease from electrolyser degradation was not mitigated by increased heat utilisation (Fig. S8 in SM). Overall, similar amounts of heat were produced from electrolysis (57 %) and methanation (43 %).

Unlike heat, the limited benefit of oxygen utilisation was not caused by demand limitations, as virtually 100 % of the oxygen produced was utilised in all configurations ($UF_{O_2} > 99.99\%$) to fulfil approximately a quarter of the oxygen demand (maximum DF_{O_2} was 26.1 %). Instead, a relatively low energy consumption of the aeration process at the investigated WWTP compared to typically assumed values (Table 1), together with the inclusion of investment costs for both aeration equipment and piping, caused negative NPV_{O_2} values in all configurations (−650 k€ in the optimised case) (Fig. S9 in SM). Although other studies [21,29] have similarly found small energy savings from electrolytic oxygen use at WWTPs, economic benefits were achieved in [29] despite the inclusion of oxygen equipment costs due to on-site use of oxygen, meaning that no piping for transportation was required and thus lower CAPEX. The impact of piping distance and aeration energy consumption on oxygen integration performance is further investigated in section 3.4. Furthermore, the impact of oxygen system scaling was limited due to the limited hydrogen demand, which prevented further oxygen production for larger systems. The minor emission reduction seen from oxygen utilisation also means that this reduction is particularly sensitive to non-operational emissions occurring during e.g. the construction phase of piping, which could counteract the operational emission reduction observed here.

3.3. System operation

The operating strategy described in section 2.4 enabled cost-optimal operation of the PtG system on a daily basis. Hydrogen storage permitted the electrolyser to overproduce during hours of low spot prices or RES generation, and to produce below demand or completely shut down when prices were high and no renewable electricity was available. The

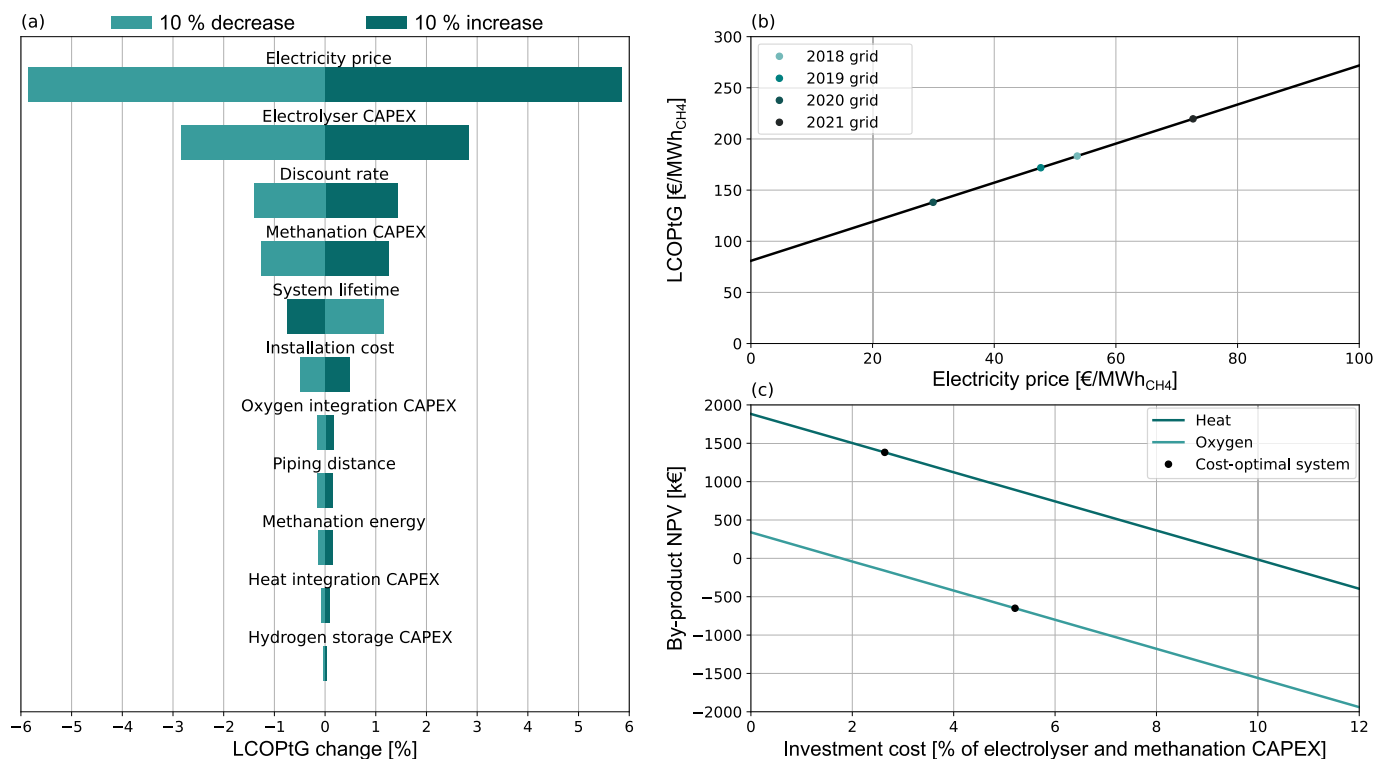


Fig. 8. Results of sensitivity analysis for (a) general parameters, (b) electricity price and (c) heat and oxygen integration capital expenditure (CAPEX).

cost-reducing effects of part load operation were reinforced by the associated increase in electrolyser efficiency. The continuous demand for hydrogen for biogas upgrading meant that electrolyser operation was fairly constant (Fig. 7a). In the optimised configuration, the electrolyser was in off or standby mode for only 0.1 % of the year, while full- and part-load operation were used for 35.2 and 64.7 % of the year, respectively. This trend was strengthened by the minor electrolyser oversizing and hydrogen storage determined through the optimisation, limiting the potential for intermittent operation, but electricity supply also had an impact as inclusion of wind power in particular encouraged continuous operation of the electrolyser (Fig. 7b). When instead driven using only grid electricity, the electrolyser was typically operated at maximum capacity during night and mid-day, when prices were low, while lower loads or complete shutdown were encouraged during mornings and evenings (Fig. S10 in SM). Similarly, systems including more PV naturally operated at high loads at midday, when PV generation reached its peak (Fig. S11 in SM). Moreover, intra-day optimisation typically resulted in the storage being emptied at the end of each day, unless there was a possibility of surplus RES generation (e.g. at the end of day 2 in Fig. 7a).

Avoided costs from by-product utilisation had little impact on actual system operation. All other things being equal, electrolyser operation would be favoured during hours when oxygen or heat could be utilised at the WWTP. However, the high aeration demand meant that hours of oxygen deficit were scarce (Fig. 7c), while the low income from oxygen utilisation further reduced the conditions during which load shifting on account of oxygen utilisation was actually feasible. In total, inclusion of oxygen in the MILP formulation increased DF_{O_2} by 0.1 % compared with excluding it for the cost-optimal case configuration. Heat utilisation provided more income and was subject to a larger, albeit still small, supply and demand mismatch. However, heat from methanation, which followed CO_2 availability and was thus independent of the electrolyser dispatch, significantly reduced the heat demand actually possible to influence through the operating strategy (Fig. 7c). Inclusion of heat utilisation in the MILP formulation increased DF_{heat} by a mere 0.03 %. However, the impact of by-product generation on system operation could be larger in a system with smaller supply and demand mismatch and more operational freedom, e.g. less RES generation and a more flexible hydrogen demand, which otherwise predominantly dictated how the system operated.

3.4. Sensitivity analysis

Sensitivity analysis was conducted to investigate the impact of parameter uncertainties on the performance of the cost-optimal system. Electricity price was most influential on LCOPTG, followed by electrolyser CAPEX (Fig. 8a). After recent increases, electrolyser costs are expected to decrease in the near future as production scales up [31,66], providing significant potential for cost reduction. A CAPEX reduction to 750 €/kW_{el} installed, in line with IEA predictions for 2030 [66], corresponded to a 43 % electrolyser CAPEX decrease in the optimal system configuration and lowered LCOPTG for the system to 170.9 €/MWh_{CH₄}. However, lower CAPEX also influenced the cost-optimal configuration itself and brought economic viability to further oversizing of the PtG system, at least when excess RES costs were not considered (section S3.1 in SM).

Fig. 8b further highlights the significance of electricity price for total LCOPTG and the variation in recent years. The study year (2021) experienced unusually high grid electricity prices compared with previous years. Although future price developments are uncertain, a return to the more typical price levels of 2018 and 2019 would reduce LCOPTG to around 170–180 €/MWh_{CH₄}. Conversely, the unusually low prices of 2020 indicate the potential cost reduction if low-cost electricity were available on a large scale. The price paid for electricity per unit hydrogen is also directly influenced by electrolyser efficiency. An increase in initial system efficiency from 75 %_{HHV} to 80 %_{HHV} reduced the

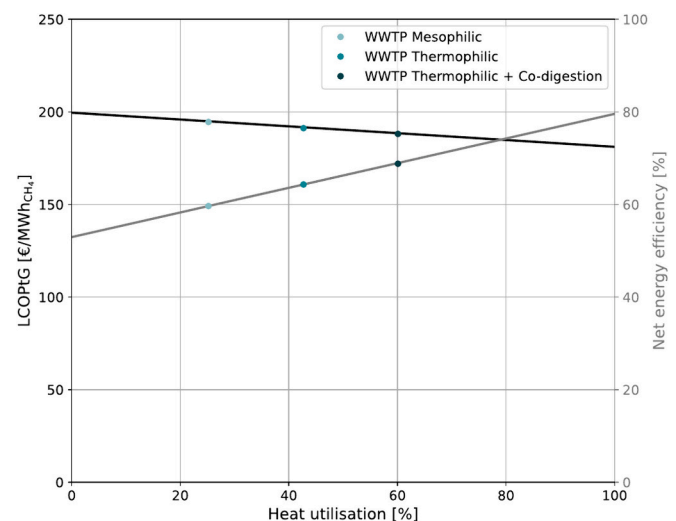


Fig. 9. Impact of heat demand on levelised cost of power-to-gas (LCOPTG) and net energy efficiency, including estimated demands for the co-digestion plant and thermophilic digestion at the wastewater treatment plant (WWTP).

total cost electricity per unit methane by 7 %, and thus reduced LCOPTG to 186.7 €/MWh_{CH₄}. Lower grid prices also influenced the cost-optimal P2G configuration and the cost reduction achievable using wind and solar, potentially requiring less RES oversizing to reach minimum LCOPTG (section S3.1 in SM).

The robustness of heat integration was evident, as NPV_{heat} remained positive until investment costs approached 10 % PtG CAPEX, nearly a fourfold increase from the study value (Fig. 8c). The low avoided costs together with the high investment costs of oxygen utilisation initially led to negative NPV_{O_2} . Positive NPV_{O_2} was achieved only when investment costs were below 2 % of PtG CAPEX, corresponding to more than a 60 % reduction. By-product NPV was influenced by the piping distance, assumed to be 1 km for the study case. This was particularly significant for oxygen utilisation, for which positive NPV could possibly be achieved for on-site use (Fig. S12 in SM). This is in line with results from [17], where a significant impact of piping distance for heat integration was found.

3.4.1. Exploration of heat utilisation potential

The performance enhancement from heat utilisation would be more significant if a larger share of the excess heat produced could be used, i.e. with greater heat demand. Considering the local case, several additional use cases for excess low-temperature heat can be found. First, anaerobic digestion at the WWTP could be changed from mesophilic to thermophilic, which would potentially double the heat demand for anaerobic digestion [84]. Biogas production could also increase and consequently the CO_2 supply, which would allow for further operation of the PtG system and additional cost reductions. Second, by switching from pasteurisation to integrated thermophilic sanitisation, the temperature level for heat utilisation in the anaerobic digester at the co-digestion plant could be reduced from 70 to 52 °C, enabling this to act as another potential PtG heat sink [5,85]. The additional heat demand from these two processes was estimated (section S3.2 in SM) and the potential effects can be seen in Fig. 9.

Increased utilisation of excess heat could improve the net system efficiency to a theoretical maximum of 79.6 %_{HHV}, or 86.2 %_{HHV} if all heat is assumed to be usable (i.e. usable heat fraction of 1). This is in line with results in a recent pilot study, where the overall efficiency of a PtG plant based on biological methanation reached 76 %_{HHV}, which could potentially be increased to 89 %_{HHV} [42]. In addition, LCOPTG could decrease to 181.1 €/MWh_{CH₄}, while net specific emissions could reach negative values using average EFs (−5.5 gCO₂/kWh_{CH₄}), indicating that

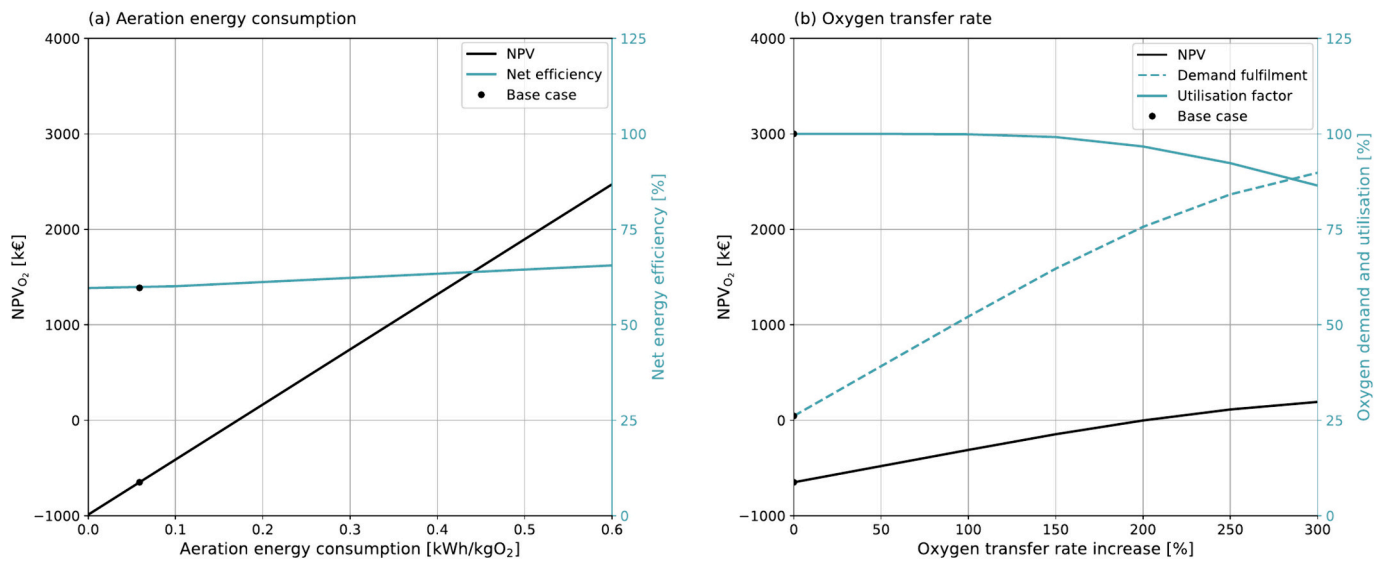


Fig. 10. Impact of (a) aeration energy consumption and (b) oxygen transfer rate on oxygen integration performance.

the emission reduction from avoided DH use exceeded that from electricity consumption, and could decrease to 623.8 gCO₂/kWh_{CH₄} using marginal factors. Full heat utilisation would be possible if e.g. the supply temperature of DH decreased at the location or if pre-heating of DH return water was conducted [16]. Solutions to increase the temperature of the waste heat and enable a wider range of utilisation options have been proposed. Heat pumps could be used to elevate the temperature of the excess heat to 100 °C or beyond [17,55]. Switching from biological to catalytic methanation, which has operating temperature in the range 200–550 °C, could also improve heat usability, although sensitivity to common biogas impurities potentially limits its use for direct methanation [15]. Higher temperature levels would enable injection into a conventional DH network [19], or heat utilisation for CO₂ capture to increase the available carbon supply [86].

Although only a minor mismatch between heat generation and demand was seen using the WWTP heat demand (0.1 %), this mismatch is likely to grow if further heat sinks are found, depending on the temporal characteristics of the additional demand. Including heat storage could be an option for ensuring complete DH independence.

3.4.2. Exploration of oxygen utilisation potential

The results from the Uppsala case suggest that oxygen integration at WWTPs may not provide economic benefits. However, since utilisation of oxygen from PtG in wastewater treatment is still a relatively unexplored topic, parameter values related to this are associated with significant uncertainty and the values assumed in this study may be conservative. Analysis of aeration energy requirement showed that oxygen integration could be economically viable in the right conditions (Fig. 10a). If the use of pure oxygen leads to substantial OTR improvements, the entire WWTP oxygen demand could potentially be met by the optimised PtG system (Fig. 10b).

Positive NPV_{O₂} was reached at aeration energy consumption above 0.17 kWh/kgO₂, which is within the typical range for Swedish WWTPs [20]. This energy consumption corresponds to an oxygen value of roughly 10 €/tO₂, just above 10 % of the average market price for oxygen in Sweden (90 €/tO₂). Hence, additional benefits may be possible through external oxygen sales if transport costs can be managed and current market prices are sustained [20]. Our values were obtained using 2021 spot prices for electricity for aeration at the WWTP. If a flat rate were used instead, NPV_{O₂} could reach zero at an electricity price of 215 €/MWh_{el}. Higher aeration energy consumption gave further efficiency improvements, and consequently emission avoidance, but had limited impact on system operation due to the already high oxygen

utilisation factor.

Under the assumption that oxygen demand did not change when using pure oxygen, i.e. that no additional OTR improvement was possible, the WWTP essentially acted as an infinite oxygen sink. However, as described in section 2.2.2, use of pure oxygen instead of air could increase OTR and thus reduce actual oxygen demand. A 300 % increase in OTR, as proposed in [28], would lead to DF_{O₂} of 89.8 % and a UF_{O₂} of 86.5 %, implying a temporal mismatch in oxygen supply and demand, and increase NPV_{O₂} to 192 k€. The UF_{O₂} value could be further increased through oxygen-based operation or storage and completely fulfil WWTP demand. Alternatively, a larger electrolyser could be installed. If the aeration demand could be fully met using pure oxygen, several additional advantages could be obtained at the WWTP, such as shorter hydraulic retention times and reduced foaming, odour and methane emissions [57]. However, the high investment cost and low energy savings, at least using the base assumptions, suggest that oxygen utilisation in WWTPs should not be the main consideration when sizing integrated PtG systems.

Another option to increase the economic potential of oxygen utilisation in wastewater treatment is ozone production for micropollutant removal [22]. If ozone treatment is already present at the facility, a switch from an air-based system to one using pure oxygen could lead to energy savings of approximately 6 kWh/kgO₃, or 0.7 kWh/kgO₂ [87]. Although the expected demand would correspond to only 12–19 % of annual oxygen production from the optimised PtG system [20], the economic case might still be improved due to the higher energy savings compared with aeration. Assuming that 15 % of the oxygen was used for ozonation generated average energy savings of 0.14 kWh/kgO₂, nearly making NPV_{O₂} positive, at least without considering any potential investment costs for ozonation.

3.5. Further benefits of an integrated system

By integrating PtG with co-digestion and wastewater treatment, coupling between the electricity, gas, heat and water sectors can be achieved. The WWTP in this study essentially acted as an infinite oxygen sink and provided heat utilisation potential which noticeably improved the techno-economic performance. Although the results in this study suggest that selling oxygen at market prices is more profitable than utilising it for aeration in WWTPs, the oxygen market might become saturated upon large-scale deployment of electrolysers, in which case prices would drop and local, low-logistics use cases would be favoured.

Use of PtG by-products at the WWTP reduced its electricity

consumption by 6 % and its overall energy consumption by 44 %. Since WWTPs typically represent around 1–5 % of national electricity consumption [21,28] and more than 1 % of global GHG emissions [23], the savings could be considerable if PtG integration were applied on a large scale, in particular for plants with less efficient aeration, or if higher OTR could be achieved using pure oxygen aeration systems and larger electricity savings can be made. Although indirect emissions from electricity consumption can be less significant than direct emissions of methane and nitrous oxide at WWTPs [88], pure oxygen utilisation may also lead to direct emission reductions [57].

Integration of PtG at biogas plants is a form of biogenic carbon capture and utilisation, where CO₂ is recycled instead of being directly emitted into the atmosphere. While CO₂ utilisation does not in itself prevent downstream emissions, it could aid in achieving negative emissions elsewhere if methane generated through this process is used in a centralised application with permanent carbon capture and storage. This could help include small-scale facilities such as biogas production, where carbon capture may not otherwise be feasible, in future carbon value chains. Access to biogenic carbon without additional cost is also an economic benefit for the PtG system. Large-scale direct air capture of atmospheric CO₂ has been estimated to cost approximately 140–375 €₂₀₂₃/tCO₂, while carbon capture from low-concentration biogenic point sources, such as power generation and industry, has an estimated cost of 60–90 €₂₀₂₃/tCO₂ [3]. A CO₂ cost would increase LCO_{PtG} by nearly 18 €/MWh_{CH₄} (9.2 %) per 100 €/tCO₂, emphasising its importance for economic viability.

Previous studies have found that the oxygen demand from wastewater treatment exceeds the CO₂ availability for methanation at WWTPs [23]. On using only the biogas produced at the WWTP (27 % of total production) in the system investigated here, approximately 69 and 9 % of the heat and oxygen demand, respectively, could be fulfilled, further demonstrating the need for additional CO₂ to meet the by-product demands. Inclusion of a co-digestion plant within the integrated system increased CO₂ availability and enabled a larger optimal PtG system, increasing by-product demand fulfilment and reducing production costs. However, CO₂ was still the limiting factor even with co-digestion included. Procuring carbon from other sources, such as the nearby biomass-driven combined heat and power plant, would thus enable further upscaling of the system and possibly enable complete oxygen demand fulfilment at the WWTP, albeit possibly with an additional CO₂ extraction cost as highlighted above.

3.6. Future outlook and research opportunities

The results of this study in the context of the Uppsala case casts doubt upon the economic feasibility of oxygen utilisation within the integrated PtG concept, which would likely prevent such systems from being realised. However, the sensitivity analysis in section 3.4 showed that our results may resemble a worst-case scenario and that specific local conditions appear to be key in determining whether electrolytic oxygen utilisation at WWTPs is economically feasible or not. Although considering the full investment cost of equipment and piping is important, optimising the configuration to reduce by-product integration CAPEX, e.g. by locating the PtG system at the WWTP to avoid expensive piping, may increase feasibility. Refurbishing of existing aeration equipment to enable pure oxygen use could produce similar benefits. In addition, WWTPs with a higher aeration energy consumption, or sites where ozonation is conducted, may be particularly suitable for this integration due to their potential for larger energy savings. It is therefore suggested that a thorough assessment of conditions at the specific site is conducted to determine the feasibility of oxygen integration before implementation. On the other hand, energy savings may also be considered sufficient to compensate for a financial loss.

The concept of integrated PtG requires further research to determine its potential. Efforts to evaluate the impact of PtG by-product utilisation in wastewater treatment would be aided by quantification of the effects

of pure oxygen on OTR in large-scale WWTPs. If OTR improvements are demonstrated to be possible on a large scale, the economic potential and thus the feasibility of the integrated concept can be improved. In addition, the concept could be applied to a co-digestion plant using integrated thermophilic sanitisation, to investigate its impact on low-temperature heat demand and CO₂ availability, as an increased heat demand was shown to have considerable benefits. A thorough life cycle assessment of the integrated system would also provide additional information regarding its environmental impacts. Furthermore, since biogas production, by-product demand and RES generation were all modelled using data from a specific location, conducting similar studies using data from other locations would increase the generalisability of the results. The identified mismatches in supply and demand between the datasets may look different in other conditions. For example, heat demand at the WWTP may be lower in warmer regions and reduce the usefulness of heat integration, while aeration energy consumption may be higher and increase the usefulness of oxygen utilisation. Although the analysed period appeared to be fairly representative of a typical year at the investigated site, the specific data is influenced by e.g. weather conditions and other time periods may thus provide slightly different outcomes even at the same location. The characteristics of the datasets used are further defined in section S2.1 in SM.

PtG by-products could provide integration options beyond those quantified in this study. Residual biomass in methanation discharge water could be redirected to the digestion tanks and increase biogas production [71]. If on-site water purification were applied, e.g. using reverse osmosis, some of the discharge water could possibly be reused in the electrolyser and reduce water consumption. The economic impact of the latter is likely small, as the cost of water was negligible, but could be important at sites with limited freshwater access.

Due to the continuous demand for hydrogen in biogas upgrading through direct methanation, which could lead to substantial operating costs during extended periods of high electricity prices, the concept could be further developed to achieve additional decoupling of electrolysis and methanation. Inclusion of buffer biogas storage, already present at some facilities [5], could e.g. make further use of the operational flexibility of biological methanation and enable full shutdown of the PtG system. Another option is the concept of flexible membrane upgrading proposed by Gantenbein et al. [89] in which a membrane, commonly used to polish the output gas from methanation, e.g. by removing residual hydrogen, could be operated either for polishing or as conventional biogas upgrading by removing CO₂. This would enable PtG upgrading when cheap electricity is available, and conventional biogas upgrading when it is not. If in-situ methanation can be realised without compromising the stability of the anaerobic digestion process, it provides another interesting flexibility option. By pairing it with conventional upgrading, in-situ methanation could be operated more intermittently than direct ex-situ methanation, while the lack of an independent methanation reactor could still reduce costs.

Although WWTPs are a readily available and, as shown in this study, promising option for integration with PtG systems, local integration possibilities can vary. Industrial processes such as pulp and paper mills provide alternative opportunities for integration of both heat and oxygen at the same facility, at least if higher temperature heat can be attained using heat pumps or high-temperature electrolysis and methanation [16]. Moreover, methanation is only one of many possibilities for CO₂ utilisation available for biogas plants. Production of other fuels and chemicals (such as methanol), materials or direct use of CO₂ in e.g. the food industry could all be viable alternatives, depending on the scale and location of the biogas plant [90]. Other types of CO₂ valorisation may lead to additional income and thus further increase the economic advantage of conventional upgrading compared to PtG observed in section 3.1.

4. Conclusions

Coupling PtG with co-digestion and wastewater treatment would provide access to biogenic CO₂ and uses for excess heat and oxygen, while replacing conventional biogas upgrading to produce low-carbon methane. In this study, a model of such an integrated system was developed and used to simulate hourly operation and optimise system configuration based on actual plant data from Uppsala, Sweden.

Optimisation of PtG components and electricity supply showed that the lowest production costs were obtained by minimising flaring of non-upgraded biogas, avoiding excessive electrolyser oversizing and, because of temporal mismatches in RES generation and biogas production, decoupling of electrolysis and the biogas production system using hydrogen storage. Depending on the value of unused renewable electricity, avoiding excess wind and solar generation could be an additional factor for cost minimisation. The cost-optimal configuration achieved LCOPtG of 194.6 €/MWh_{CH₄}, net energy efficiency of 59.7 %_{HHV} and net specific emissions of 37.2 and 635.2 gCO₂/kWh_{CH₄} in an average and marginal perspective, respectively. Significant cost savings could be made if investment and grid electricity costs decrease from current high levels and through valorisation of unused RES generation. Replacing biogas upgrading with PtG was shown to require a methane sales price above 180 €/MWh_{CH₄} to improve economic performance.

The analysis highlighted both the promise and potential restrictions of integrating PtG by-products within wastewater treatment. In the investigated case, by-product utilisation increased system efficiency by 7.4 %-units and consequently lowered production costs by 1.0 % and emissions from average and marginal perspectives by 28.3 and 2.2 %, respectively. Heat integration accounted for most of the performance improvement, while oxygen integration provided only minor positive effects on efficiency and emissions, and slightly increased overall production costs. The limited impact of oxygen integration was demonstrated to depend on site-specific conditions, i.e. a relatively low energy consumption of the aeration process in the investigated system and high investment costs due to piping distances. Its feasibility could therefore improve for WWTPs with higher electricity consumption, pure oxygen aeration systems with increased oxygen transfer efficiency, or on-site oxygen use. Furthermore, the optimised system had overproduction of heat, fulfilling the heat demand using 25.2 % of heat generated, but underproduction of oxygen, fulfilling only 26.1 % of the oxygen demand using all available oxygen. Thus, larger benefits may be realised if additional heat sinks are found. Owing to the difference in magnitude of by-product supply and demand, temporal mismatches due to non-complementary biogas production and wastewater flows were insignificant and by-product utilisation had virtually no impact on system operation.

CRedit authorship contribution statement

Linus Engstam: Writing – original draft, Visualization, Software, Methodology, Formal analysis, Data curation, Conceptualization. **Leandro Janke:** Writing – review & editing, Supervision, Funding acquisition, Conceptualization. **Cecilia Sundberg:** Writing – review & editing, Supervision, Conceptualization. **Åke Nordberg:** Writing – review & editing, Supervision, Funding acquisition, Conceptualization.

Declaration of competing interest

The authors declare that they have no known competing financial interests or personal relationships that could have appeared to influence the work reported in this paper.

Data availability

A GitHub link has been provided in the supplementary material through which the model developed can be downloaded.

Acknowledgements

The study was funded by the Swedish Energy Agency within the Biogas Solutions Research Center (grant number 52669-1), and within the ERA-Net Smart Energy Systems Project “Power-2-Transport” (grant agreement 775970), which are gratefully acknowledged. In addition, the authors thank co-digestion and wastewater treatment plant operators at Uppsala Vatten for their valuable provision of plant data.

Appendix A. Supplementary data

Supplementary data to this article can be found online at <https://doi.org/10.1016/j.apenergy.2024.124534>.

References

- [1] European Commission. The European Green Deal [Online]. Available: <https://eur-lex.europa.eu/legal-content/EN/TXT/?uri=CELEX:52019DC0640>; 2019.
- [2] IPCC. Climate Change 2022. In: Shukla PR, Skea J, Slade R, Al Khouradje A, van Diemen R, McCollum D, Pathak M, editors. Mitigation of Climate Change. Contribution of Working Group III to the Sixth Assessment Report of the Intergovernmental Panel on Climate Change; 2022 [Online]. Available: https://report.ipcc.ch/ar6/wg3/IPCC_AR6_WGIII_Full_Report.pdf.
- [3] IEA. CCUS in clean energy transitions. Paris. [Online]. Available: <https://www.iea.org/reports/ccus-in-clean-energy-transitions>; 2020.
- [4] Zhang X, Witte J, Schildhauer T, Bauer C. Life cycle assessment of power-to-gas with biogas as the carbon source. *Sustain Energy Fuels* Mar. 2020;4(3):1427–36. <https://doi.org/10.1039/c9se00986h>.
- [5] Calbry-Muzyka AS, Schildhauer TJ. Direct Methanation of biogas—technical challenges and recent Progress. *Front Energy Res Dec.* 2020;8:356. <https://doi.org/10.3389/fenrg.2020.570887>.
- [6] Sterner M, Specht M. Power-to-gas and power-to-X—the history and results of developing a new storage concept. *Energies* Oct. 2021;14(20):6594. <https://doi.org/10.3390/en14206594>.
- [7] Ramsebner J, Haas R, Ajanovic A, Wietschel M. The sector coupling concept: a critical review. *Wiley Interdiscip Res Energy Environ* Jul. 2021;10(4):e396. <https://doi.org/10.1002/wene.396>.
- [8] Rusmanis D, O’Shea R, Wall DM, Murphy JD. Biological hydrogen methanation systems—an overview of design and efficiency. *Bioengineered* Jan. 2019;10(1):604–34. <https://doi.org/10.1080/21655979.2019.1684607>.
- [9] Vo TQ, Wall DM, Ring D, Rajendran K, Murphy JD. Techno-economic analysis of biogas upgrading via amine scrubber, carbon capture and ex-situ methanation. *Appl Energy* Feb. 2018;212:1191–202. <https://doi.org/10.1016/j.apenergy.2017.12.099>.
- [10] Goffart De Roeck F, Buchmayr A, Gripekoven J, Mertens J, Dewulf J. Comparative life cycle assessment of power-to-methane pathways: process simulation of biological and catalytic biogas methanation. *J Clean Prod* Dec. 2022;135033. <https://doi.org/10.1016/j.jclepro.2022.135033>.
- [11] Gorre J, Ruoss F, Karjunen H, Schaffert J, Tynjälä T. Cost benefits of optimizing hydrogen storage and methanation capacities for power-to-gas plants in dynamic operation. *Appl Energy* Jan. 2020;257:113967. <https://doi.org/10.1016/j.apenergy.2019.113967>.
- [12] Collet P, Flottes E, Favre A, Raynal L, Pierre H, Capela S, et al. Techno-economic and life cycle assessment of methane production via biogas upgrading and power to gas technology. *Appl Energy* 2017;192:282–95. <https://doi.org/10.1016/j.apenergy.2016.08.181>.
- [13] Thapa A, Jo H, Han U, Cho SK. Ex-situ biomethanation for CO₂ valorization: state of the art, recent advances, challenges, and future prospective. *Biotechnol Adv* Nov. 2023;68. <https://doi.org/10.1016/j.biotechadv.2023.108218>.
- [14] Gantenbein A, Kröcher O, Biollaz SMA, Schildhauer TJ. Techno-economic evaluation of biological and fluidised-bed based Methanation process chains for grid-ready biomethane production. *Front Energy Res* 2022;9:775259. <https://doi.org/10.3389/fenrg.2021.775259>.
- [15] Götz M, et al. Renewable power-to-gas: a technological and economic review. *Renew Energy* 2016;85:1371–90. <https://doi.org/10.1016/j.renene.2015.07.066>.
- [16] Saxe M, Alvfors P. Advantages of integration with industry for electrolytic hydrogen production. *Energy* Jan. 2007;32(1):42–50. <https://doi.org/10.1016/j.energy.2006.01.021>.
- [17] van der Roest E, Bol R, Fens T, van Wijk A. Utilisation of waste heat from PEM electrolyzers – unlocking local optimisation. *Int J Hydrogen Energy* Apr. 2023;48(72):27872–91. <https://doi.org/10.1016/j.ijhydene.2023.03.374>.
- [18] Michailos S, Walker M, Moody A, Poggio D, Pourkashanian M. Biomethane production using an integrated anaerobic digestion, gasification and CO₂ biomethanation process in a real waste water treatment plant: a techno-economic assessment. *Energy Convers Manage* Apr. 2020;209:112663. <https://doi.org/10.1016/j.enconman.2020.112663>.
- [19] Böhm H, Moser S, Puschnigg S, Zauner A. Power-to-hydrogen & district heating: technology-based and infrastructure-oriented analysis of (future) sector coupling potentials. *Int J Hydrogen Energy* Sep. 2021;46(63):31938–51. <https://doi.org/10.1016/j.ijhydene.2021.06.233>.

- [20] Gustavsson M., et al. Potential use and market of oxygen as a by-product from hydrogen production. *Energiforsk* 2023;937. [Online]. Available: <https://energiforsk.se/program/vatgasens-roll-i-energi-och-klimatostallningen/rapporter/potential-use-and-market-of-oxygen-as-a-by-product-from-hydrogen-production-2023-937/>.
- [21] Campana PE, Mainardis M, Moretti A, Cottes M. 100% renewable wastewater treatment plants: techno-economic assessment using a modelling and optimization approach. *Energy Convers Manage* Jul. 2021;239:114214. <https://doi.org/10.1016/j.enconman.2021.114214>.
- [22] Schäfer M, Gretzschel O, Steinmetz H. The possible roles of wastewater treatment plants in sector coupling. *Energies* Apr. 2020;13(8):2088. <https://doi.org/10.3390/en13082088>.
- [23] Rusmanis D, Yang Y, Lin R, Wall DM, Murphy JD. Operation of a circular economy, energy, environmental system at a wastewater treatment plant. *Adv Appl Energy* Dec. 2022;8:100109. <https://doi.org/10.1016/j.adapen.2022.100109>.
- [24] O'Shea R, Wall DM, McDonagh S, Murphy JD. The potential of power to gas to provide green gas utilising existing CO₂ sources from industries, distilleries and wastewater treatment facilities. *Renew Energy* 2017;114(B):1090–100. <https://doi.org/10.1016/j.renene.2017.07.097>.
- [25] Rusmanis D, et al. Electrofuels in a circular economy: a systems approach towards net zero. *Energy Convers Manage* Sep. 2023;292:117367. <https://doi.org/10.1016/j.enconman.2023.117367>.
- [26] Michailos S, Walker M, Moody A, Poggio D, Pourkashanian M. A techno-economic assessment of implementing power-to-gas systems based on biomethanation in an operating waste water treatment plant. *J Environ Chem Eng* Feb. 2021;9(1):104735. <https://doi.org/10.1016/j.jece.2020.104735>.
- [27] Csédy Z, Sinóros-Szabó B, Zavarkó M. Seasonal energy storage potential assessment of WWTPs with power-to-methane technology. *Energies* 2020;13(18):4973. <https://doi.org/10.3390/en13184973>.
- [28] Donald R, Love JG. Energy shifting in wastewater treatment using compressed oxygen from integrated hydrogen production. *J Environ Manage* Apr. 2023;331:117205. <https://doi.org/10.1016/j.jenvman.2022.117205>.
- [29] Hönig F, Rupakula GD, Duque-Gonzalez D, Ebert M, Blum U. Enhancing the Levelized Cost of Hydrogen with the Usage of the Byproduct Oxygen in a Wastewater Treatment Plant. *Energies* 2023;16(12):4829. Jun. 2023, <https://doi.org/10.3390/en16124829>.
- [30] Buttler A, Spliethoff H. Current status of water electrolysis for energy storage, grid balancing and sector coupling via power-to-gas and power-to-liquids: a review. *Renew Sustain Energy Rev* 2018;82:2440–54. <https://doi.org/10.1016/j.rser.2017.09.003>.
- [31] IRENA. Green Hydrogen Cost Reduction [Online]. Available: https://www.irena.org/-/media/Files/IRENA/Agency/Publication/2020/Dec/IRENA_Green_hydrogen_cost_2020.pdf; 2020.
- [32] Cummins. HyLYZER Water Electrolyzers [Online]. Available: <https://www.cummins.com/sites/default/files/2021-08/cummins-hylyzer-1000-specsheet.pdf>; 2020.
- [33] Ginsberg MJ, Venkatraman M, Esposito DV, Fthenakis VM. Minimizing the cost of hydrogen production through dynamic polymer electrolyte membrane electrolyzer operation. *Cell Reports Phys Sci* Jun. 2022;3(6):100935. <https://doi.org/10.1016/j.xcrp.2022.100935>.
- [34] Hydrogen Nel. The World's Most Efficient and Reliable Electrolysers [Online]. Available: https://nelhydrogen.com/wp-content/uploads/2020/03/Electrolysers-Brochure_PD-0600-0125-Rev-E.pdf; 2024.
- [35] Kopp M, Coleman D, Stiller C, Scheffer K, Aichinger J, Schepat B. Energiepark Mainz: technical and economic analysis of the worldwide largest power-to-gas plant with PEM electrolysis. *Int J Hydrogen Energy* 2017;42(19):13311–20. <https://doi.org/10.1016/j.ijhydene.2016.12.145>.
- [36] H-TEC Systems. H-TEC PEM Electrolyser ME450/1400. <https://www.h-tec.com/en/products/detail/h-tec-pem-electrolyser-me450/me450/>; 2024. accessed Jan. 27, 2024.
- [37] ICCT. Assessment of Hydrogen Production Costs from Electrolysis: United States and Europe [Online]. Available: https://theicct.org/sites/default/files/publications/final_icct2020_assessment_of_hydrogen_production_costs_v2.pdf; 2020.
- [38] Parra D, Valverde L, Pino FJ, Patel MK. A review on the role, cost and value of hydrogen energy systems for deep decarbonisation. *Renew Sustain Energy Rev* 2019;101:279–94. <https://doi.org/10.1016/j.rser.2018.11.010>.
- [39] Zauner A, Böhm H, Rosenfeld DC, Tichler R. Innovative large-scale energy storage technologies and Power-to-Gas concepts after optimization: D7.7 Analysis on future technology options and on techno-economic optimization [Online]. Available: <https://ec.europa.eu/research/participants/documents/downloadPublic?documentId=08016665c58ae3ff&appId=PPGMS>; 2019.
- [40] Langmi HW, Engelbrecht N, Modisha PM, Bessarabov D. Hydrogen storage. *Electrochem Power Sources Fundam Syst Appl Hydrog Prod by Water Electrolysis* Jan. 2022:455–86. <https://doi.org/10.1016/b978-0-12-819424-9.00006-9>.
- [41] Electrochaea. Power-to-Gas via Biological Catalysis (P2G-Biocat) [Online]. Available: https://energiforskning.dk/sites/energiteknologi.dk/files/slutrapport_r/12164_final_report_p2g_biocat.pdf; 2014.
- [42] Schlautmann R, et al. Renewable power-to-gas: a technical and economic evaluation of three demo sites within the STORE&GO project. *Chemie-Ingenieur-Technik* Apr. 2021;93(4):568–79. <https://doi.org/10.1002/cite.202000187>.
- [43] Bellini R, et al. Biological aspects, advancements and techno-economic evaluation of biological Methanation for the recycling and valorization of CO₂. *Energies* Jun. 2022;15(11):4064. <https://doi.org/10.3390/en15114064>.
- [44] Mørs F, Schlautmann R, Jachin Gorre, Leonhard R. Innovative large-scale energy storage technologies and power-to-gas concepts after optimisation. D5.9: Final report on evaluation of technologies and processes [Online], https://www.storean.dgo.info/fileadmin/downloads/deliverables_2020/20200713-STOREandGO_D5.9_DVGW_Final_report_on_evaluation_of_technologies_and_processes.pdf; 2020.
- [45] Kirchbacher F, Miltner W, Wukovits W, Harasek M. Economic assessment of membrane-based power-to-gas processes for the European biogas market. *Renew Sustain Energy Rev* Sep. 2019;112:338–52. <https://doi.org/10.1016/j.rser.2019.05.057>.
- [46] Engstam L, Janke L, Sundberg C, Nordberg Å. Grid-supported electrolytic hydrogen production: cost and climate impact using dynamic emission factors. *Energy Convers Manage* 2023;293. <https://doi.org/10.1016/j.enconman.2023.117458>.
- [47] Vattenfall AB. EPD ® of Electricity from Vattenfall's Wind Farms Vattenfall AB - EPD Registration number: S-P-01435 [Online]. Available: <https://api.environdec.com/api/v1/EPDLibrary/Files/487ba9dd-8cca-4c17-cd8a-08d9df0ea78f/Data>; 2022.
- [48] Hong S, Qvist S, Brook BW. Economic and environmental costs of replacing nuclear fission with solar and wind energy in Sweden. *Energy Policy* Jan. 2018;112:56–66. <https://doi.org/10.1016/j.enpol.2017.10.013>.
- [49] Tranberg B, Corradi O, Lajoie B, Gibon T, Staffell I, Andresen GB. Real-time carbon accounting method for the European electricity markets. *Energy Strat Rev* Nov. 2019;26:100367. <https://doi.org/10.1016/j.esr.2019.100367>.
- [50] Bosmans JHC, Dammeier LC, Huijbregts MAJ. Greenhouse gas footprints of utility-scale photovoltaic facilities at the global scale. *Environ Res Lett* 2021;16(9). <https://doi.org/10.1088/1748-9326/ac1df9>.
- [51] Jordan DC, Kurtz SR, VanSant K, Newmiller J. Compendium of photovoltaic degradation rates. *Prog Photovoltaics Res Appl* Jul. 2016;24(7):978–89. <https://doi.org/10.1002/ppp.2744>.
- [52] Shinde AM, Dikshit AK, Odlare M, Thorin E, Schwede S. Life cycle assessment of bio-methane and biogas-based electricity production from organic waste for utilization as a vehicle fuel. *Clean Technol Environ Policy* Aug. 2021;23(6):1715–25. <https://doi.org/10.1007/s10098-021-02054-7>.
- [53] Feiz R, Johansson M, Lindkvist E, Moestedt J, Pålédal SN, Ometto F. The biogas yield, climate impact, energy balance, nutrient recovery, and resource cost of biogas production from household food waste—a comparison of multiple cases from Sweden. *J Clean Prod* Dec. 2022;378. <https://doi.org/10.1016/j.jclepro.2022.134536>.
- [54] Vattenfall. Fjärrvärme i Uppsala. <https://www.vattenfall.se/foretag/fjarrvarme/sa-fungerar-fjarrvarme/vara-orter/upsala/>; 2024. accessed Jan. 17, 2024.
- [55] Mantei F, Kraume M, Salem O. Improved energy efficiency of power-to-X processes using heat pumps towards mobility sector Defossilization. *Chem Ing Tech* 2022. <https://doi.org/10.1002/CITE.202200118>.
- [56] Tiktak WJ. Heat Management of PEM Electrolysis [Master's thesis, Delft University of Technology]. Available: <http://resolver.tudelft.nl/uuid:c046820a-72bc-4f05-b72d-e60a3ecb8c89>; 2019.
- [57] Mohammadpour H, Cord-Ruwisch R, Pivrikas A, Ho G. Utilisation of oxygen from water electrolysis – assessment for wastewater treatment and aquaculture. *Chem Eng Sci* Dec. 2021;246:117008. <https://doi.org/10.1016/j.ces.2021.117008>.
- [58] Steinmetz H. Oxygen from Electrolysis for Wastewater Treatment [Online]. Available: <https://wastewater2023.eap.gr/wp-content/uploads/2023/07/Steinmetz-H.-presentation.pdf>; 2023.
- [59] Drenowski J, Remiszewska-Skwarek A, Duda S, Łagód G. Aeration process in bioreactors as the main energy consumer in a wastewater treatment plant. Review of solutions and methods of process optimization. *Processes* 2019;7(5). <https://doi.org/10.3390/pr7050311>.
- [60] Staffell I, Pfenninger S. Using bias-corrected reanalysis to simulate current and future wind power output. *Energy* Nov. 2016;114:1224–39. <https://doi.org/10.1016/j.energy.2016.08.068>.
- [61] Pfenninger S, Staffell I. Long-term patterns of European PV output using 30 years of validated hourly reanalysis and satellite data. *Energy* Nov. 2016;114:1251–65. <https://doi.org/10.1016/j.energy.2016.08.060>.
- [62] Energiforsk. El från nya anläggningar [Online]. Available: <https://energiforsk.se/media/30970/el-fra-nya-anla-ggningar-energiforskrapport-2021-714.pdf>; 2021.
- [63] Baumhof MT, Raheli E, Johnsen AG, Kazempour J. Optimization of Hybrid Power Plants: When Is a Detailed Electrolyzer Model Necessary? [Online]. Available: <https://arxiv.org/abs/2301.05310v1>; Jan. 2023.
- [64] Wirtz M, Hahn M, Schreiber T, Müller D. Design optimization of multi-energy systems using mixed-integer linear programming: which model complexity and level of detail is sufficient? *Energy Convers Manage* 2021;240:114249. <https://doi.org/10.1016/j.enconman.2021.114249>.
- [65] Thema M, et al. Biological CO₂-methanation: an approach to standardization. *Energies* May 2019;12(9):1670. <https://doi.org/10.3390/en12091670>.
- [66] International Energy Agency. Global Hydrogen Review 2023 [Online]. Available: <https://www.iea.org/reports/global-hydrogen-review-2023>; 2023.
- [67] Böhm H, Zauner A, Rosenfeld DC, Tichler R. Projecting cost development for future large-scale power-to-gas implementations by scaling effects. *Appl Energy* Apr. 2020;264:114780. <https://doi.org/10.1016/j.apenergy.2020.114780>.
- [68] Reksten AH, Thomassen MS, Møller-Holst S, Sundseth K. Projecting the future cost of PEM and alkaline water electrolyzers; a CAPEX model including electrolyser plant size and technology development. *Int J Hydrogen Energy* Nov. 2022;47(90):38106–13. <https://doi.org/10.1016/j.ijhydene.2022.08.306>.
- [69] Parnellos E, Zun MT, McLellan BC. Cost projection of global green Hydrogen production scenarios. *Hydrog* Nov. 2023;4(4):932–60. <https://doi.org/10.3390/hydrogen4040055>.
- [70] Reuß M, Grube T, Robinus M, Preuster P, Wasserscheid P, Stolten D. Seasonal storage and alternative carriers: a flexible hydrogen supply chain model. *Appl Energy* Aug. 2017;200:290–302. <https://doi.org/10.1016/j.apenergy.2017.05.050>.

- [71] Lardon L, Thorberg D, Krosgaard L. WP3 – Biogas valorization and efficient energy management (Technical and economic analysis of biological methanation) [Online]. Available: <http://www.powerstep.eu/system/files/generated/files/resource/d3-2-technical-and-economic-analysis-of-biological-methanationdeliverable.pdf>; 2018.
- [72] Varela C, Mostafa M, Zondervan E. Modeling alkaline water electrolysis for power-to-x applications: a scheduling approach. *Int J Hydrogen Energy* 2021;46(14): 9303–13. <https://doi.org/10.1016/j.ijhydene.2020.12.111>.
- [73] Moretti L, Astolfi M, Vergara C, Macchi E, Pérez-Arriaga JI, Manzolini G. A design and dispatch optimization algorithm based on mixed integer linear programming for rural electrification. *Appl Energy* 2019;233–234:1104–21. <https://doi.org/10.1016/j.apenergy.2018.09.194>.
- [74] Maluenda M, Córdova S, Lorca Á, Negrete-Pincetic M. Optimal operation scheduling of a PV-BESS-Electrolyzer system for hydrogen production and frequency regulation. *Appl Energy* 2023;344:121243. <https://doi.org/10.1016/j.apenergy.2023.121243>.
- [75] IEA. The role of E-fuels in Decarbonising transport. Paris. [Online]. Available: <https://www.iea.org/reports/the-role-of-e-fuels-in-decarbonising-transport>; 2023.
- [76] Ali Khan MH, et al. Designing optimal integrated electricity supply configurations for renewable hydrogen generation in Australia. *iScience* Jun. 2021;24(6):102539. <https://doi.org/10.1016/j.isci.2021.102539>.
- [77] Kapica J, Canales FA, Jurasz J. Global atlas of solar and wind resources temporal complementarity. *Energ Conver Manage* Oct. 2021;246:114692. <https://doi.org/10.1016/j.enconman.2021.114692>.
- [78] Lindberg O, Lingfors D, Arnqvist J. Analyzing the mechanisms behind temporal correlation between power sources using frequency separated time scales: a Swedish case study on PV and wind. *Energy* Nov. 2022;259:124817. <https://doi.org/10.1016/j.energy.2022.124817>.
- [79] European Commission. Commission Delegated Regulation (EU) 2023/1184 of 10 February 2023 supplementing Directive (EU) 2018/2001 of the European Parliament and of the Council by establishing a Union methodology setting out detailed rules for the production of renewable liquid and gaseous transport fuels of non-biological origin [Online]. Available: http://data.europa.eu/eli/reg_del/2023/1184/oj; 2023.
- [80] Carbon Price Tracker. <https://ember-climate.org/data/data-tools/carbon-price-viewer/>; 2024. accessed Apr. 17, 2024.
- [81] Martin J, Dimanchev E, Neumann A. Carbon abatement costs for renewable fuels in hard-to-abate transport sectors. *Adv Appl Energy* Dec. 2023;12:100156. <https://doi.org/10.1016/j.adapen.2023.100156>.
- [82] Reiter G, Lindorfer J. Global warming potential of hydrogen and methane production from renewable electricity via power-to-gas technology. *Int J Life Cycle Assess* 2015;20:477–89. <https://doi.org/10.1007/s11367-015-0848-0>.
- [83] Parra D, Zhang X, Bauer C, Patel MK. An integrated techno-economic and life cycle environmental assessment of power-to-gas systems. *Appl Energy* 2017;193:440–54. <https://doi.org/10.1016/j.apenergy.2017.02.063>.
- [84] Zupancič GD, Roš M. Heat and energy requirements in thermophilic anaerobic sludge digestion. *Renew Energy* Nov. 2003;28(14):2255–67. [https://doi.org/10.1016/S0960-1481\(03\)00134-4](https://doi.org/10.1016/S0960-1481(03)00134-4).
- [85] Grim J, Malmros P, Schnürer A, Nordberg Å. Comparison of pasteurization and integrated thermophilic sanitation at a full-scale biogas plant – heat demand and biogas production. *Energy* Jan. 2015;79(C):419–27. <https://doi.org/10.1016/j.energy.2014.11.028>.
- [86] Coppitters D, et al. Energy, exergy, economic and environmental (4E) analysis of integrated direct air capture and CO₂ methanation under uncertainty. *Fuel* Jul. 2023;344:127969. <https://doi.org/10.1016/j.fuel.2023.127969>.
- [87] Peyrelasse C, Jacob M, Lallement A. Multicriteria comparison of ozonation, membrane filtration, and activated carbon for the treatment of recalcitrant organics in industrial effluent: a conceptual study. *Environ Process Mar.* 2022;9(1): 1–21. <https://doi.org/10.1007/s40710-022-00563-1>.
- [88] Parravicini V, Svardal K, Krampe J. Greenhouse gas emissions from wastewater treatment plants. *Energy Procedia* Nov. 2016;97:246–53. <https://doi.org/10.1016/j.egypro.2016.10.067>.
- [89] Gantenbein A, Witte J, Biollaz SMA, Kröcher O, Schildhauer TJ. Flexible application of biogas upgrading membranes for hydrogen recycle in power-to-methane processes. *Chem Eng Sci* Jan. 2021;229:116012. <https://doi.org/10.1016/j.ces.2020.116012>.
- [90] Cordova SS, Gustafsson M, Eklund M, Svensson N. What should we do with CO₂ from biogas upgrading? *J CO₂ Util* Nov. 2023;77:102607. <https://doi.org/10.1016/j.jcou.2023.102607>.